ESA CONTRACT REPORT

Contract Report to the European Space Agency

Experimental assimilation of radar measurements

August 2010

Authors: M. Janisková

WP-3200 report for ESA contract 1-5576/07/NL/CB:
Project QuARL - Quantitative Assessment of the Operational Value of Space-Borne Radar and Lidar Measurements of Cloud and Aerosol Profiles

European Centre for Medium-Range Weather Forecasts
Europäisches Zentrum für mittelfristige Wettervorhersage
Centre européen pour les prévisions météorologiques à moyen terme

ECMWF

Series: ECMWF - ESA Contract Report

A full list of ECMWF Publications can be found on our web site under:
http://www.ecmwf.int/publications/

Contact: library@ecmwf.int

European Centre for Medium-Range Weather Forecasts
Shinfield Park, Reading, RG2 9AX, England

Contract Report to the European Space Agency

Experimental assimilation of radar measurements

Authors: M. Janisková

WP-3200 report for ESA contract 1-5576/07/NL/CB:
Project QuARL - Quantitative Assessment of the Operational Value of Space-Borne Radar and Lidar Measurements of Cloud and Aerosol Profiles

European Centre for Medium-Range Weather Forecasts
Shinfield Park, Reading, Berkshire, UK

August 2010

ABSTRACT

Observations providing three-dimensional information on clouds from spaceborne active instruments on board of CloudSat and CALIPSO are already available and new ones, such as EarthCARE, should appear in the near future. This opens new possibilities to explore the usefulness of this data sources not only directly for model parametrization improvements, but also to investigate their usage in the assimilation process which could transform a possible extracted information from the data through the model into an improvement of the initial atmospheric state. In this study, a 1D+4D-Var technique has been selected to study the impact of observations related to clouds on 4D-Var (four-dimensional variational) analyses and subsequent forecasts. Using this two step approach, temperature and specific humidity profiles retrieved from 1D-Var assimilation of CloudSat observations have been included in the 4D-Var system. Several experiments have been run for a couple of selected meteorological situations and the statistical evaluation of the results has been carried out.

Contents

1 Introduction **1**

2 Methodology **2**

2.1 Description of the 1D+4D-Var approach . . . 2

2.1.1 4D-Var system . . . 3

2.1.2 1D-Var system . . . 3

2.1.3 Background error statistics . . . 3

3 Experimental framework **4**

3.1 Observations and observation errors in the 1D-Var system . . . 4

3.2 Pseudo-observations and their errors used in 4D-Var . . . 4

4 1D+4D-Var experiments for CloudSat observations **5**

4.1 Experimental setup . . . 5

4.2 Situations used in experimentation . . . 6

4.3 Results . . . 6

4.3.1 Situation on 24 April 2008 over USA . . . 6

4.3.2 Situation on 16 September 2007 - tropical cyclone . . . 22

5 Conclusion and perspectives **32**

A List of Acronyms **34**

1 Introduction

Numerical weather prediction (NWP) models have improved considerably over the past few years in the forecast of clouds thanks to progress in parametrizations. However, there is still need to explore new possibilities for model improvement through assimilation of data related to clouds from active and passive sensors. Observations providing three-dimensional information on clouds from space-borne active instruments on board of CloudSat and CALIPSO (Cloud-Aerosol Lidar and Infrared Pathfinder Satellite Observations) are already available and new ones, such as EarthCARE (Earth, Clouds, Aerosols and Radiation Explorer) should appear in the near future. The challenge is to identify information that can be extracted from such data sources and transformed through the model into knowledge about the atmospheric state.

In WP-3100 of the QuARL project, feasibility studies have been performed for the definition of an assimilation system for measurements obtained from nadir-pointing radar/lidar instruments (measurements with small spatial coverage, but high vertical resolution). Those studies have been done using a 1D-Var (one-dimensional variational) approach since it was recognize that it would be difficult to start an investigation of using these new types of observations in the framework of the full 4D-Var (four-dimensional variational) assimilation system (operationally used at ECMWF), which is very complex and thus quite difficult to interpret. A 1D-Var system has been built for the assimilation of CloudSat reflectivities (level-1 product), as well as for the retrieved cloud liquid and ice water contents (level-2 products). In addition, the CloudSat profile observations have also been combined with MODIS cloud optical depth in the assimilation process.

To study the impact of the above mentioned new observations on 4D-Var analyses and subsequent forecasts, a 1D+4D-Var technique has been selected. This two-stage approach has been used operationally for assimilation of precipitation related observations (Bauer *et al.*, 2006a,b) at ECMWF from June 2005 to June 2008. Before that, the benefits of such method had been demonstrated for rain rate observations by Marécal and Mahfouf (2000, 2002). It has also proven to be successful in early implementation of clear-sky infrared radiance assimilation in the past (e.g. Eyre *et al.*, 1993; Phalippou, 2005) and for SSM/I brightness temperatures in clear-sky areas (Gérard and Saunders, 1999). The application of the 1D+4D-Var technique to assimilate observations from the Tropical Rainfall Measuring Mission (TRMM) precipitation radar by Benedetti *et al.* (2006) has shown that active sensor data can provide useful information on the moisture field which can be assimilated to improve the analysis and the forecast of tropical disturbances.

Section 2 introduces the 1D+4D-Var technique applied to the assimilation of cloud observations from CloudSat and briefly summarizes the observation operators and the background error statistics used in this study. Details of the set-up for assimilation experiments are given in section 3. Results from the 1D+4D-Var experiments are introduced and discussed in section 4. Finally, section 5 provides a summary and draws the conclusions of this study.

2 Methodology

2.1 Description of the 1D+4D-Var approach

In the past years, a 1D+4D-Var approach has been developed for assimilation of rain rates or rain-affected radiances at ECMWF. This two-step strategy will be used in this study to assimilate CloudSat observations and it is schematically described in Fig. 2.1. In the first step, a 1D-Var assimilation technique is used to assimilate CloudSat reflectivities (level-1 products) or retrieved cloud liquid and ice water contents (level-2 products). The CloudSat observations are averaged over the model grid-box with T799 spectral resolution (corresponding to approximately 25 km). The 1D-Var assimilation is performed with the aim of adjusting the model temperature and specific humidity profiles. An evaluation of specific humidity and temperature analysis increments performed in WP-3100 (Development of strategies for radar and lidar assimilation) has shown that both variables are modified by the assimilation of cloud related observations and therefore pseudo-observations of specific humidity and temperature profiles from 1D-Var retrievals should be used instead of the total column water vapour (TCWV) used in the 1D-Var+4D-Var approach for precipitation observations (Bauer *et al.*, 2006a,b). The second step consists of the assimilation of these 1D-Var retrieval products into the 4D-Var system as pseudo-observations.

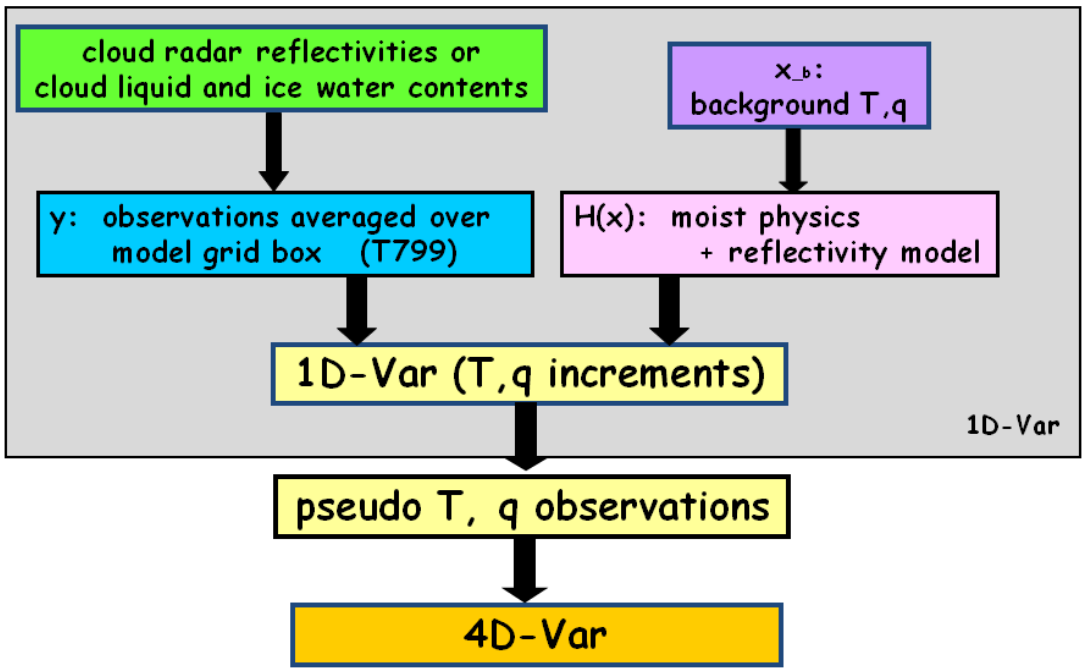

Figure 2.1: *Schematic description of 1D+4D-Var technique.*

2.1.1 4D-Var system

Since November 1997 the operational data assimilation system at ECMWF is a four-dimensional variational (4D-Var) system (Rabier *et al.*, 2000; Mahfouf and Rabier, 2000). This system is based on the incremental formulation proposed by Courtier *et al.* (1994).

4D-Var seeks an optimal balance between observations and the dynamics of the atmosphere by finding a model trajectory $\mathbf{x}(t)$ which is as close as possible, in a least-square sense, to the observations available during a given time period $[t_0, t_n]$. The model trajectory $\mathbf{x}(t)$ is completely defined by the initial state $\mathbf{x}_0$ at time t_0.

The misfit to given observations $\mathbf{y}^o$ and to an *a-priori* model state $\mathbf{x}^b$ called background, which is usually provided by a short-range forecast, is measured by an objective cost-function defined as:

$$\mathscr{J}(\mathbf{x}_0) = \frac{1}{2}(\mathbf{x}_0 - \mathbf{x}_0^b)^T \mathbf{B}^{-1}(\mathbf{x}_0 - \mathbf{x}_0^b) + \frac{1}{2}\sum_{i=0}^{n}(H_i[\mathbf{x}(t_i)] - \mathbf{y}_i^o)^T \mathbf{R}_i^{-1}(H_i[\mathbf{x}(t_i)] - \mathbf{y}_i^o) \tag{2.1}$$

where at any time t_i,

- $\mathbf{y}_i^o$ is the vector of observations;
- $\mathbf{x}_0^b$ is the background model state at the initial time and in the current 4D-Var system it consists of temperature, humidity, vorticity, divergence and surface pressure;
- H_i is the operator providing the equivalent of the observed data from the model variable $\mathbf{x}(t_i)$, it also describes the spatial interpolations to observation locations and the action of the forecast model to propagate the initial state $\mathbf{x}_0$ to the time of each observation;
- $\mathbf{R}_i$ is the observation error covariance matrix (including measurement and representativeness errors);
- $\mathbf{B}$ is the background error covariance matrix of the state $\mathbf{x}^b$ and is based on a wavelet formulation (Fisher, 2004) to introduce regime-dependent error statistics.

2.1.2 1D-Var system

The principle of the 1D-Var is similar to that of 4D-Var, but the control vector $\mathbf{x}$ represents a single column only and the time dimension is not included. Only temperature and specific humidity are included in the 1D-Var control vector $\mathbf{x}_0$.

In the assimilation of cloud properties, the observation operator H consists of two simplified parametrizations of moist atmospheric processes: a convection scheme (Lopez and Moreau, 2005) and a cloud scheme simulating large-scale condensation and precipitation processes
(Tompkins and Janisková, 2004). When cloud radar reflectivity observations are assimilated, it also includes the radar forward model (described in WP-1000 and briefly in WP-3100) to convert model fields into reflectivities. Input cloud and precipitation fields to the radar forward model (ZmVar - reflectivity model for variational assimilation) are computed by the moist physics parametrisations whose main input variables are temperature and humidity.

2.1.3 Background error statistics

The specification of the background error covariance matrix $\mathbf{B}$ is an important aspect of the variational analysis since the information from observations is distributed in the vertical primarily through this matrix. For the 1D-Var assimilation of cloud observations, the covariance matrix of the background errors is taken from

the operational ECMWF 4D-Var system and described in more detail in WP-3100. No cross correlations between the background errors of specific humidity and temperature are considered. In 4D-Var, background error correlations are modified by adding a wavelet decomposition for introducing spatial inhomogeneity (Fisher, 2004).

3 Experimental framework

1D-Var assimilation experiments have been performed offline using different CloudSat observations. Background values have been taken from a 12-hour forecast of the ECMWF model with T799 spectral truncation (corresponding to approximately 25 km) and 91 vertical levels. The forecast results have been stored every half an hour in order to use observations in 1D-Var in the same way as in the operational 4D-Var system where all observations are split into half-hour time slots. The profiles of temperature (T) and specific humidity (q), along with surface pressure (p_s), tendencies, and surface quantities have first been used in the moist physics routines (simplified convection and cloud schemes described above) to compute cloud properties (cloud cover, ice and liquid-water contents) and precipitation fluxes. When assimilating reflectivities, a radar observation operator has then been applied to the model fields to obtain the equivalent model reflectivity. Specific humidity and temperature profiles retrieved from offline 1D-Var assimilation have then been used as pseudo-observations to be included into the 4D-Var system in order to study the impact of the new observations on 4D-Var analyses and subsequent forecasts.

3.1 Observations and observation errors in the 1D-Var system

Measurements of cloud radar reflectivity, converted to $\mathrm{mm}^6\ \mathrm{m}^{-3}$ (level-1 product), or the cloud liquid and ice water contents in $\mathrm{kg\ m}^{-3}$ (level-2 products) from the CloudSat 94 GHz radar have been used in these feasibility studies based on the outcome of work package WP-3100.

The impact of any type of observations in data assimilation is partly determined by the errors that are assigned to them. These errors should take into account not only instrumental error, but also representativeness error and observation operator error. As a first approach to error definition, the error on observed reflectivities has been fixed to 25% of the observed values at all levels. Observation errors for the derived cloud liquid and ice water contents have been used as percentage from the contents themselves as defined in the CloudSat level-2 products. In order to account in some way for the representativeness problem related to the small spatial coverage of CloudSat measurements, the errors for these observations have been increased depending on the CloudSat scene variability product (based on MODIS data). It is important to mention that observation errors for the reflectivities are not equivalent to observation errors for the derived cloud liquid and ice water contents. Therefore 1D-Var can be driven to observations in different ways for level-1 and level-2 products. As a consequence, there can be a larger/smaller impact on either T or q at different levels, depending on the type of assimilated observations.

3.2 Pseudo-observations and their errors used in 4D-Var

The performed 1D-Var assimilation experiments have revealed that the assimilated cloud related observations have modified both control variables of the 1D-Var system, i.e. temperature and specific humidity, as shown by the size of analysis increments. Therefore it was decided that pseudo-observations of temperature (T) and specific humidity (q) profiles retrieved from 1D-Var should be included in the 4D-Var system. Some technical developments in the ECMWF 4D-Var system were required in order to recognize

these profile observations. Previously only vertically integrated pseudo-observations of total column water vapour had been used operationally in a 1D-Var+4D-Var approach for precipitation assimilation. The new pseudo-observations have only been used above 0.5 km elevation and up to approximately 20 km, i.e. in the vertical extent where CloudSat observations are available for 1D-Var retrievals. Though specific humidity and temperature increments could be present below and above those levels, they would not be constrained by the observations but rather come from the background error covariance in matrix **B**.

The determination of T and q observation errors is not straightforward since these pseudo-observations come from the 1D-Var retrievals and therefore the observation errors correspond to the 1D-Var retrieval errors. These depend on the background error assumed for the 1D-Var control variables, the observation errors (either for reflectivity or for cloud liquid and ice water contents) and the accuracy of the observation operator used by the 1D-Var system. As originally shown by Rodgers (2000) and later used in 1D+4D-Var approaches described by Bauer *et al.* (2006b), Benedetti *et al.* (2006) or Lopez and Bauer (2007), the error on the retrieved variables can be directly derived from the 1D-Var analysis error covariance matrix, **A**, defined as follows:

$$\mathbf{A} = \left[\mathbf{B}^{-1} + \mathbf{K}^T(\mathbf{x})\ \ \mathbf{R}^{-1}\ \ \mathbf{K}(\mathbf{x})\right]^{-1} \tag{3.1}$$

where $\mathbf{K} = \left[\frac{\partial H(\mathbf{x})}{\partial \mathbf{x}}\right]$ represents the Jacobian matrix of the partial derivatives of the 1D-Var observation operator, H, with respect to the control variable, $\mathbf{x}$. This error computation could be influenced by the problem of possible non-linearity of the observation operator. However, based on the convergence performance of 1D-Var system, it seems that the linearity of the observation operator is ensured for the majority of the cases. The dimension of the observation vector is quite high using profiling observations and the computation of error is quite expensive even when using the adjoint to derive the Jacobian matrix. However, due to the lack of other error estimation options, Eq. 3.1 has been used in the non-operational feasibility studies performed in this project.

The errors for T and q produced by Eq. 3.1 are around 0.5 K for temperature and vary from 7 to around 50% of pseudo-observation value itself for specific humidity. They are on average approximately twice as small as the errors used for radiosonde temperature and specific humidity measurements. Since the observation errors influence the impact of observations in data assimilation, experiments have also been performed with inflated errors compared to those which were directly derived from Eq. 3.1.

4 1D+4D-Var experiments for CloudSat observations

Several 4D-Var experiments have been run for two different selected meteorological situations using T and q pseudo-observations retrieved from 1D-Var assimilation of CloudSat observations.

4.1 Experimental setup

The following assimilation experiments have been run:

- **ref** - reference run, i.e. run without pseudo-observations included in 4D-Var system,
- **refl** - 4D-Var experiment assimilating T and q pseudo-observations retrieved from 1D-Var with cloud radar reflectivity, using observation errors derived from the 1D-Var analysis covariance matrix (Eq. 3.1),
- **refl2err** - same as **refl**, but using observation errors twice as large as the computed ones,
- **refl1.5err** - same as **refl**, but using observation errors 1.5 times as large as the computed ones (only for the situation on 24 April 2008),

- **liwc** - 4D-Var experiment assimilating T and q pseudo-observations retrieved from 1D-Var with cloud liquid and ice water contents, using observation errors as derived from the 1D-Var analysis covariance matrix,
- **liwc2err** - same as **liwc**, but using observation errors twice as large as the computed ones.

1D+4D-Var assimilation experiments with CloudSat observations have been run over one assimilation cycle for the selected cases and 10-day forecasts have been run from the analyses to study the impact of these new observations on 4D-Var analyses and subsequent forecasts. The reference (control) 4D-Var run has been carried out over 10 days in order to obtain reference analyses which could be used for the verification of the forecasts from the different 1D+4D-Var assimilation experiments.

4.2 Situations used in experimentation

Two situations among those already used in 1D-Var assimilation studies performed in WP-3100 (Development of strategies for radar and lidar data assimilation) have been selected for 1D+4D-Var experimentations. The selected situations are:

- **20080424** - the track between 19:13 and 19:23 UTC on 24 April 2008 over a cloud system (with precipitation in its middle) over the USA,
- **20070916** - the track between 4:48 and 4:54 UTC on 16 September 2007 crossing a tropical cyclone in the west Pacific.

4.3 Results

4.3.1 Situation on 24 April 2008 over USA

The satellite track for the situation on 24 April 2008 between 19:13 and 19:23 UTC is displayed in Fig. 4.1. It crosses over a cloud system above the USA and it is covered by 193 model grid points. This situation has been selected since there is some precipitation in the centre of the system (Fig. 4.9 - 4.10) and therefore allows us to use the NEXRAD (NEXt-generation RADar) precipitation data as additional independent observations for the validation of our experiments. These data come from NCEP stage IV radar and gauge precipitation analysis with 4-km resolution and hourly accumulation (Baldwin and Mitchell, 1996; Fulton *et al.*, 1998). Figure 4.1 (right) also shows observational data coverage over the domain in the vicinity of the CloudSat satellite track. In this area, there is a large amount of conventional and satellite observations which were used by the 4D-Var system. Therefore to obtain a significant impact from T, q pseudo-observations may not be easy as 4D-Var is already well constrained by all other existing observations over the domain.

Results from different assimilation experiments (described in subsection 4.1) are provided in Fig. 4.2 - 4.12 and Tables 4.1 - 4.2.

(a) Comparisons of the first-guess and analysis against assimilated observations

The statistical evaluation of the 1D+4D-Var performance has been done for all performed experiments.

Probability distribution functions (PDF) of first-guess (FG) departures (first-guess minus observations) and analysis (AN) departures (analysis minus observations) for the pseudo-observations of temperature are shown in Fig. 4.2. PDFs for specific humidity are in Fig. 4.3. The PDFs of the first-guess departures for temperature are very similar whether the T, q pseudo-observations have been retrieved from 1D-Var of

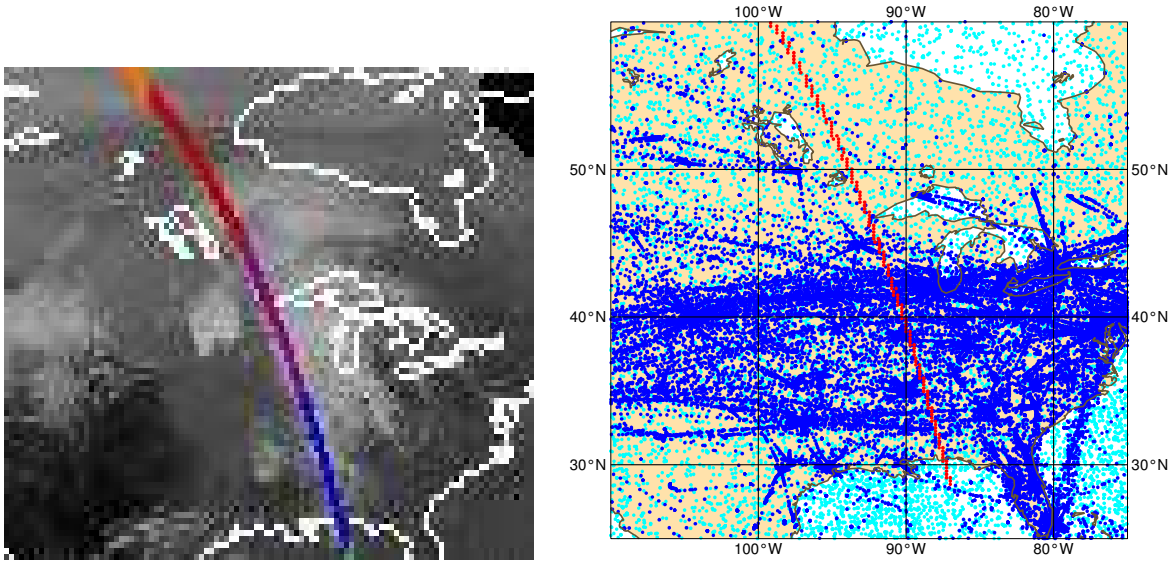

Figure 4.1: *Satellite image of situation on 24 April 2008 over USA (left) and data coverage over the domain used in 4D-Var assimilation system (right): conventional observations (dark blue), satellite observations (cyan) and pseudo-observations from 1D-Var (red).*

cloud radar reflectivity or cloud liquid and ice water contents. For specific humidity, there are slight differences for the FG departures between -0.5 and 0.5 g kg^{-1} and there are more cases with departures close to zero for **liwc** experiments than for **refl** experiments. But overall similarities of the departures indicate a consistency of the retrieved T, q from 1D-Var using either level-1 (cloud radar reflectivity) or level-2 products (cloud liquid and ice water contents). When looking at the analysis departures, one can notice that using larger errors for the pseudo-observations leads to more narrow PDFs of the analysis departures, especially noticeable for T. Generally, PDFs of analysis departures become more narrow compared to the PDFs of FG departures, indicating that the analyses are getting closer to these observations. This is also confirmed by Table 4.1 containing bias and standard deviation (stdv) of the first-guess and analysis departures for the different assimilation experiments described in subsection 4.1. Standard deviations are slightly smaller for the experiments with larger pseudo-observation errors.

Two-dimensional PDFs of analysis-minus-observation versus background-minus-observation (Fig. 4.4 for temperature and Fig. 4.5 provide information about the 4D-Var performance in a more illustrative way. They can show more clearly whether the new cloud observations can more easily dry the model than moisten it and they also allows us to see more differences between performances of the different assimilation experiments. The flatter the distribution of shaded areas around the x-axis (indicating frequency of departure occurrence) is, the better 4D-Var performs. This is also indicated by the line corresponding to the mode of the analysis departure distribution for each background departure class being closer to the x-axis. However, one must be aware that this is only true when the distribution width is narrow at the same time. Otherwise, the mode line could also be close to the x-axis when AN departures are not changed with respect to FG departures and the PDF distribution is Gaussian. From this type of statistics, one can see that the system is generally more efficient at modifying temperature than specific humidity. The situation under study includes large areas covered by precipitating clouds and hence the atmospheric state is close to or at saturation. In such a situation clouds can be modified mostly (or sometimes only) by modifying T. Temperature increments for all performed experiments seem to be quite symmetric since T is decreased and increased with similar frequency. There is more asymmetry for q analysis increments, this is especially obvious for all **refl** experiments. Using new observations in 4D-Var can more easily reduce specific humidity than increase

it. 1D+4D-Var with pseudo-observations retrieved from the 1D-Var of cloud liquid and ice water contents provides more symmetric q increments. It is possible to see that the assimilation experiments with larger errors for the pseudo-observations (2 or 1.5 times) than those derived from the 1D-Var analysis covariance matrix (Eq. 3.1) perform better since they provide a flatter departure distribution. It seems that experiments with larger observation errors "fight" less with other observations, i.e. using errors comparable to other T, q observations, helps in limiting the amount of noise that would be introduced by constraining the 4D-Var towards one kind of observations only and thus reducing the analysis departures more. This indicates that possible overfit to observations when observation errors are too small leads to sub-optimal analysis. Among the five experiments performed for this study, **liwc2err** experiment has the smallest analysis departures and the most symmetric distribution for positive and negative departures for both temperature and specific humidity.

Information about the vertical structure of the model departures from assimilated observations is provided in Fig. 4.6 and 4.7 displaying profiles of T, q bias and standard deviation for the first-guess and analysis departures from the different 4D-Var experiments. From these figures it is obvious that the vertical profiles of bias and standard deviation for the FG departures, especially for T, are very consistent for the pseudo-observations coming from 1D-Var with either cloud radar reflectivities or cloud liquid and ice water contents. This confirms the consistency of the retrieved T, q using level-1 or level-2 CloudSat products already seen in the PDFs (Fig. 4.2, 4.4). There are only noticeable differences in the vertical profiles of specific humidity bias between **refl** and **liwc** experiments. In the vertical profiles, it is more difficult to judge whether experiments with the larger observation errors have smaller AN departures, except for **liwc** where the signal of better performance is more noticeable. Otherwise AN departures on the vertical are very similar for all performed assimilation experiments.

Verification of the assimilation runs has also been done against other assimilated observation types for the domain over the Eastern USA (25°N-65°N and 105°W-85°W). Generally, no significant changes have appeared when considering observations-minus-background and observation-minus-analysis departure statistics for all types of observations assimilated in 4D-Var over the selected domain. There was one noticeable improvement in meridional wind (v-wind component) mainly in the experimental assimilation runs as verified against conventional radiosonde measurements (TEMP), aircraft weather reports (AIREP) and upper-wind reports from land stations (PILOT). An example is provided in Fig. 4.8 for PILOT observations of zonal and meridional wind for **refl2err** assimilation experiment compared to the reference (**ref**) run. The bias and the standard deviation of the departures for the meridional wind is reduced at most levels in **refl2err** compared to **ref**. The reduction is larger between 450 and 700 hPa and even stronger around 200 hPa. It should be mentioned that achieving a significant difference between the reference run and the different experimental runs over a given domain well covered by a large amount of other measurements is not easy. However, one could deteriorate the fit to the observations by including T, q pseudo-observations. This indeed happened when the pseudo-observations were accidentally included into 4D-Var system with the wrong longitude definition causing to use a mirror image of the data track (not shown).

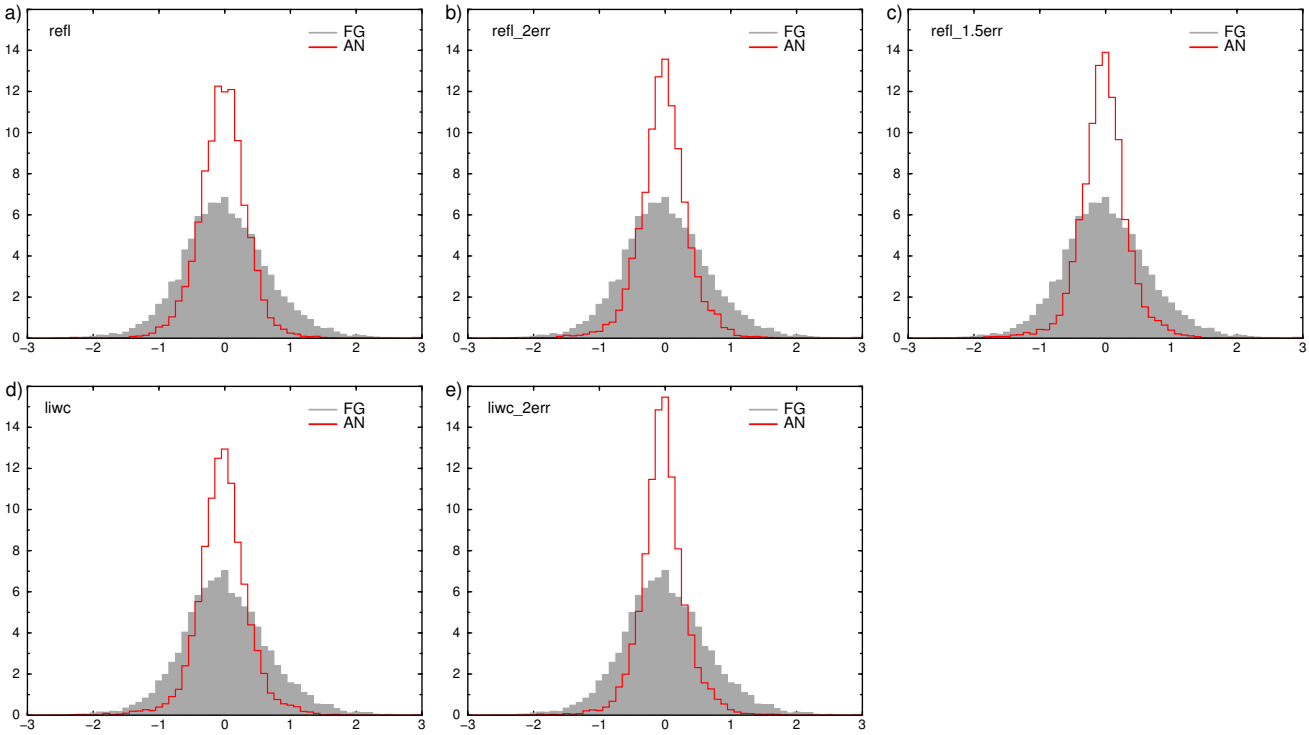

Figure 4.2: *Probability distribution function (PDF) of first-guess (grey shading) and analysis (red line) departures for temperature (K) from different 4D-Var experiments assimilating T and q pseudo-observations retrieved from 1D-Var with cloud radar reflectivity (a-c) or cloud liquid and ice water contents (d-e) using observation errors as derived from the 1D-Var analysis covariance matrix (a,d), twice as large (b,e) and 1.5 times as large (c) as the computed ones. Case of 24 April 2008 over the USA.*

	T		q	
	bias	stdv	bias	stdv
FG-refl	0.015	0.672	0.0007	0.3992
AN-refl	-0.035	0.388	0.0206	0.2955
AN-rel2err	-0.023	0.389	0.0155	0.2943
AN-refl1.5err	-0.031	0.381	0.0155	0.2836
FG-liwc	0.016	0.674	-0.0039	0.3729
AN-liwc	-0.003	0.397	-0.0004	0.2793
AN-liwc2err	-0.003	0.355	-0.0026	0.2788

Table 4.1: *Bias and standard deviation (stdv) of the first-guess (FG) and analysis (AN) departures for the different assimilation experiments (see text for experiment description). FG-refl departures are from the experiment when pseudo-observations were retrieved from 1D-Var with cloud radar reflectivity and FG-liwc when retrieved from 1D-Var with cloud liquid and ice water contents. 193 profiles were included in the statistics for the case of 24 April 2008 over the USA.*

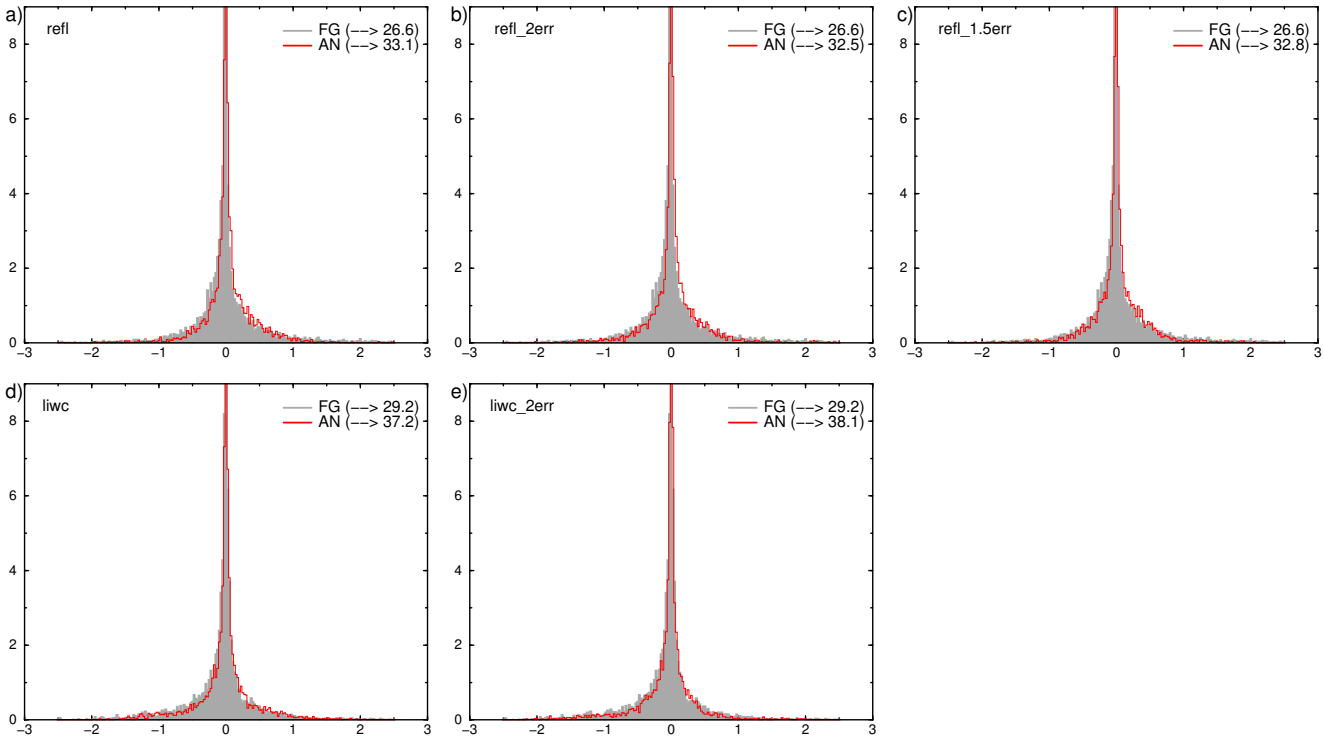

Figure 4.3: *Same as Fig. 4.2, but for specific humidity (g kg^{-1}).*

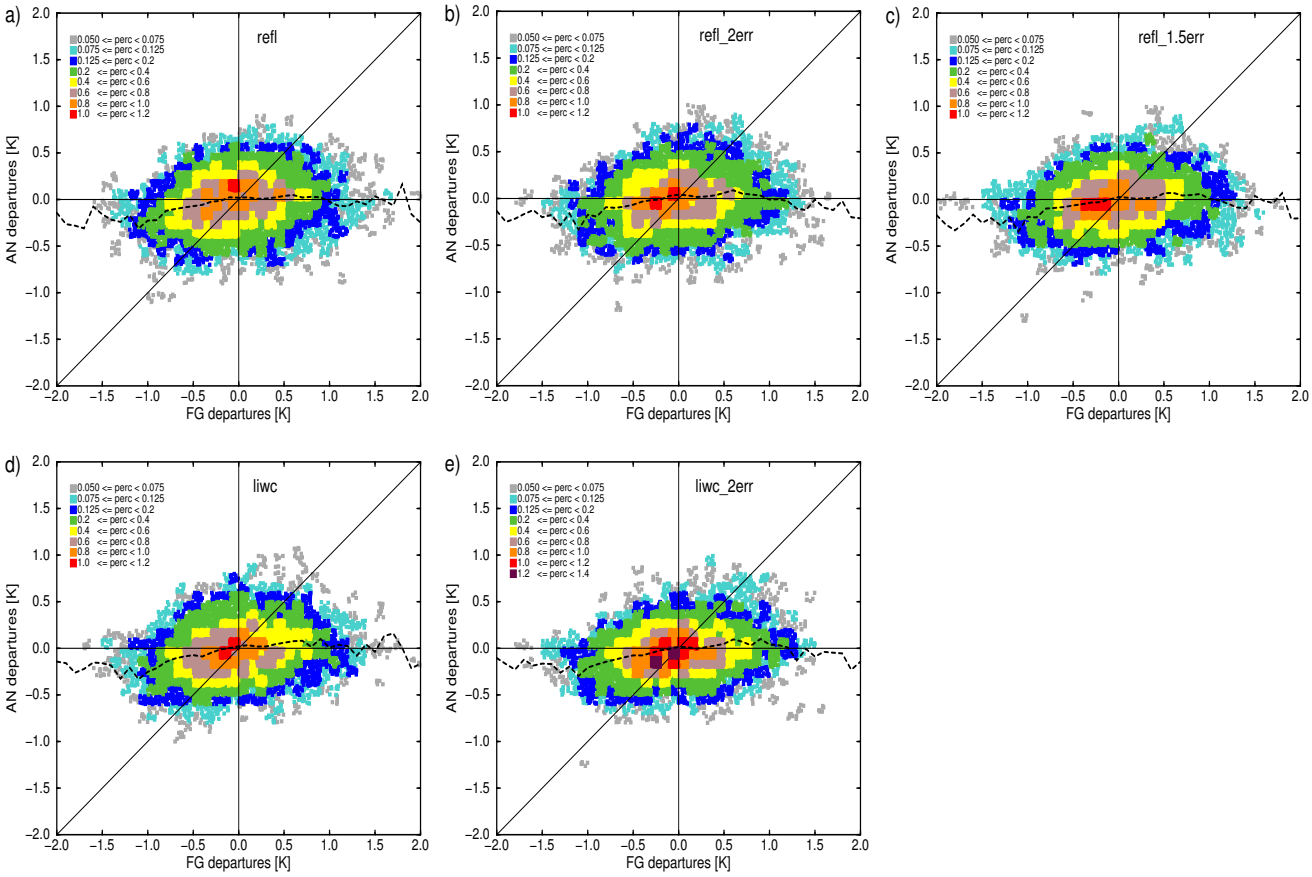

Figure 4.4: *2D PDF of analysis-minus-observation versus background-minus-observation departures for temperature (K) from different 4D-Var experiments assimilating T and q pseudo-observations retrieved from 1D-Var with cloud radar reflectivity (a-c) or cloud liquid and ice water contents (d-e) using observation errors as derived from the 1D-Var analysis covariance matrix (a,d), twice as large (b,e) and 1.5 times as large (c) as the computed ones. Colour shading indicates frequency in % while the black dashed line corresponds to the mode of the analysis departure distribution for each background departure class. Case of 24 April 2008 over the USA.*

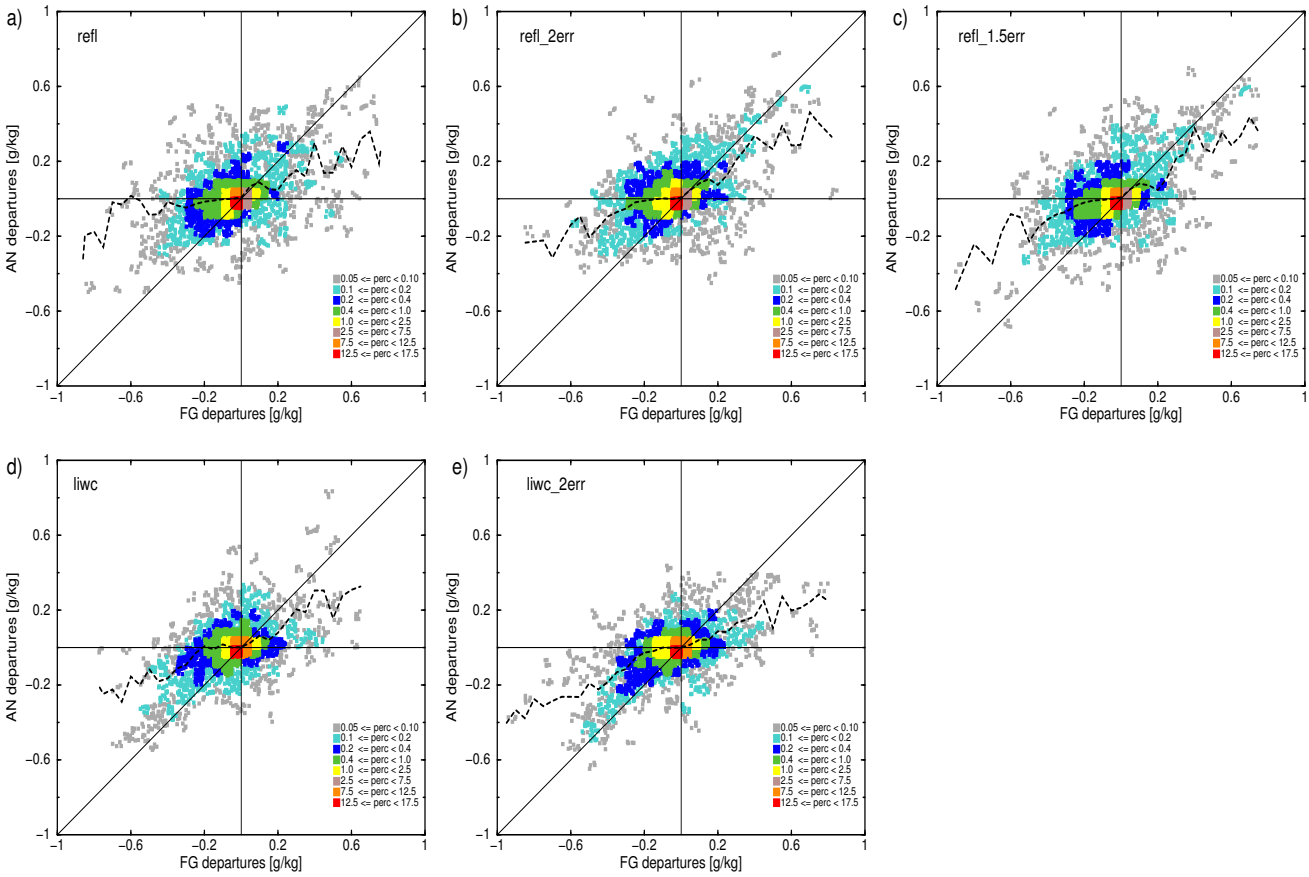

Figure 4.5: *Same as Fig. 4.4, but for specific humidity (g kg^{-1}).*

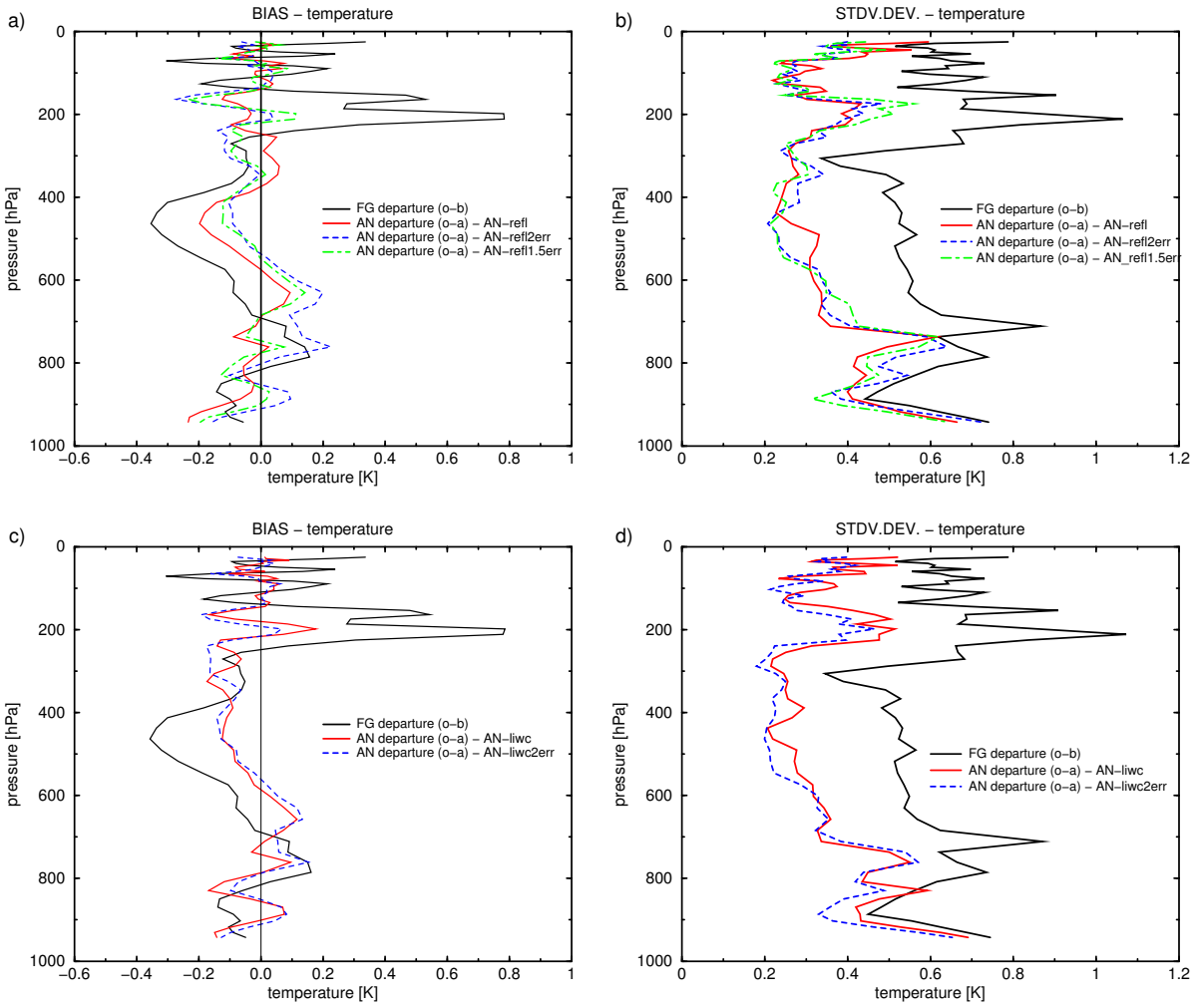

Figure 4.6: *Profiles of temperature (in K) bias (a,c) and standard deviation (b,d) for the first guess (black solid line) and analysis departures (different colour lines as explained by figure legends) from different 4D-Var experiments assimilating T and q pseudo-observations retrieved from 1D-Var with cloud radar reflectivity (top) or cloud liquid and ice water contents (bottom). Case of 24 April 2008 over the USA.*

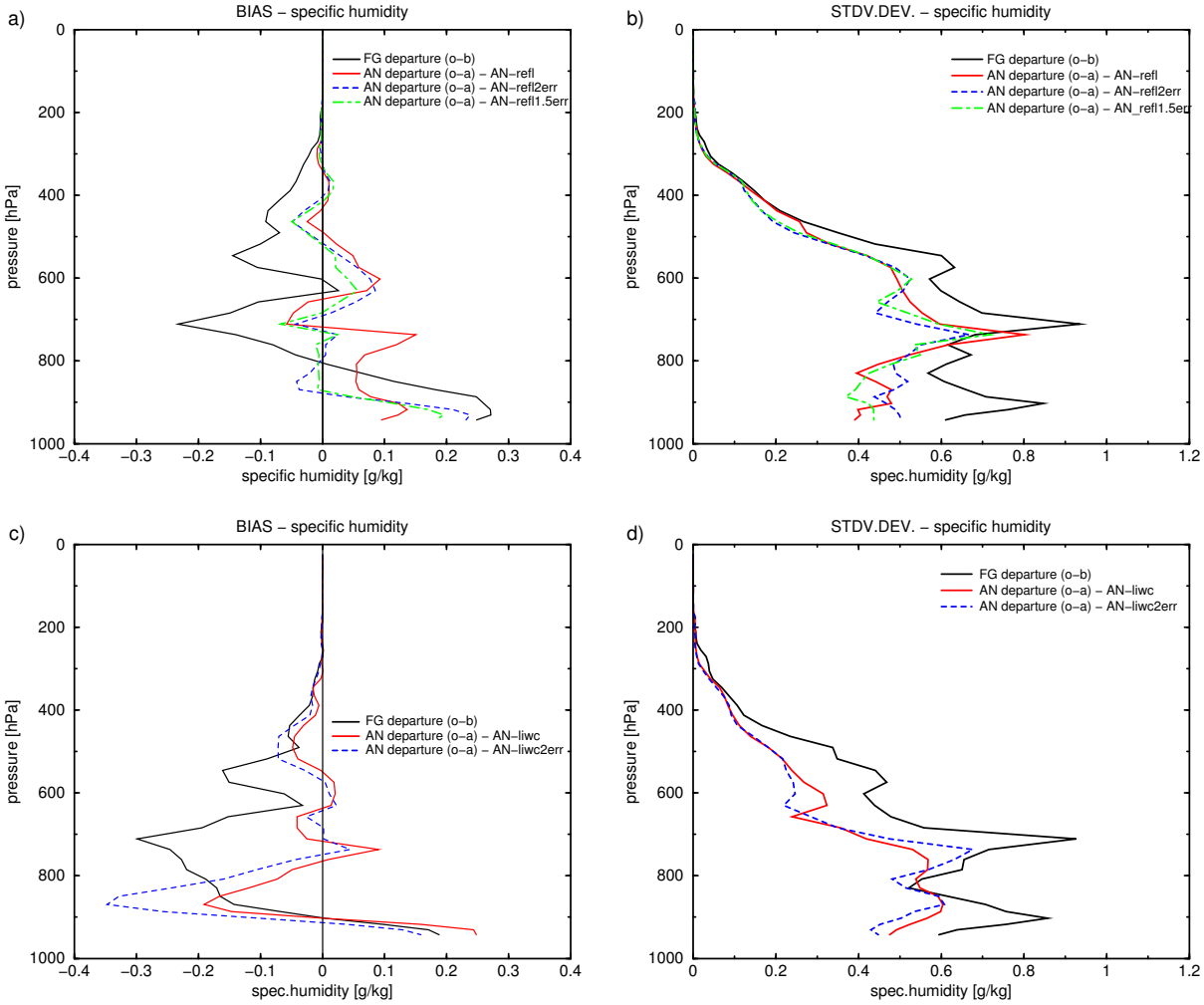

Figure 4.7: *Same as Fig. 4.6, but for specific humidity (g kg^{-1}).*

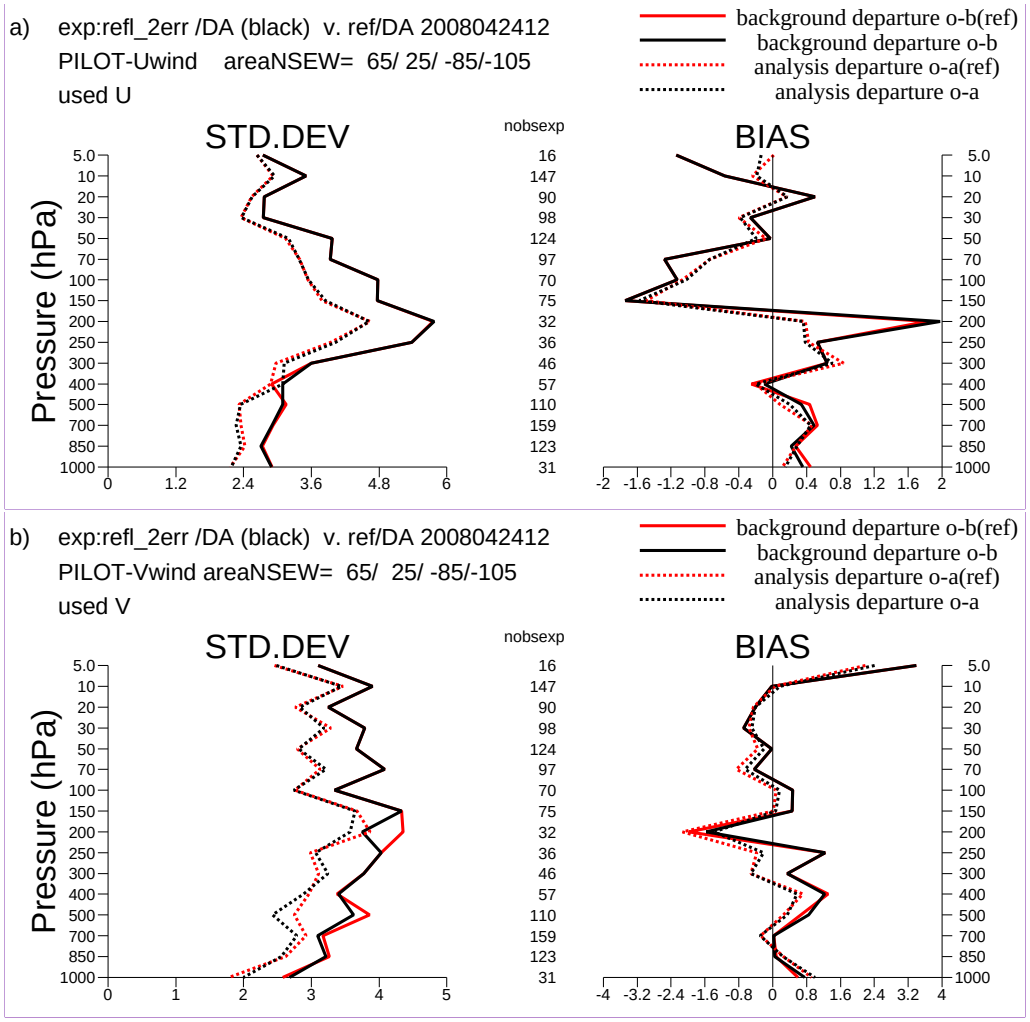

Figure 4.8: *Standard deviation (left) and bias (right) of background departures (solid line) and analysis departures (dotted line) with respect to PILOT observations of (a) zonal wind and (b) meridional wind for the reference experiment (red) and for 4D-Var experiment assimilating T and q pseudo-observations retrieved from 1D-Var with cloud radar reflectivity using observation errors twice as large as the computed ones from the 1D-Var analysis covariance matrix. Number of observations (nobsexp) over the USA for the situation on 24 April 2008 is displayed in the middle. Vertical axis shows pressure in hPa.*

(b) Impact of 1D+4D-Var assimilation on the subsequent forecast

To validate the performed assimilation experiments it is important to use independent observations (i.e. observations which were not assimilated in the system). One example of such observations is the NEXRAD precipitation data set, which was used to validate the short-range precipitation forecasts from the different assimilation experiments. Figure 4.9 shows the impact (expressed as $\overline{|obs-exp|-|obs-ref|}$) on 3-hour accumulated precipitation between t+6- and t+9-hour forecasts starting from analyses on 24 April 2008 at 12:00 UTC created by the different 4D-Var experiments (exp) assimilating T and q pseudo-observations when compared to the reference run (ref). Positive (resp. negative) impact is shown with blue (resp. red) shadings. The track of CloudSat pseudo-observations is also included in the figure (blue solid line). The 3-hour period for the precipitation accumulation (from 19:00 to 21:00 UTC) is the closest 3-hourly accumulation period to the time when the new observations (the track between 19:13 and 19:23 UTC) were included into the 4D-Var system. Though the mean impact is close to zero, there is an improvement in the precipitation amount in the middle of the precipitation area (also middle of the pseudo-observation track) which is consistent for all experiments, just having different intensities. Some improvement is also possible to see on the edges of precipitation pattern which is more spread to the south in the reference run than indicated by the NEXRAD precipitation data. The experimental runs are clearing/reducing precipitation mostly south of the precipitating area, as well as on the east (**refl**) or west (**liwc2err**) sides. To quantify which experiment provides the best precipitation forecast closer to the observations, correlation coefficients between observations and the model data have been computed for 3-hour accumulated precipitation up to 12 hours (Table 4.2). This has been done over domain A (30°N-51°N and 100°W-85°W) and for the period between the t+9 and t+6-hour forecasts also over the smaller domain B (30°N-51°N and 94°W-87°W) as displayed on Fig. 4.9. The highest correlation has been achieved by the **refl1.5err** experiment (followed closely by **refl2err**), consistently for all time periods shown in the table. Decreased correlation with respect to the reference run is mostly seen in the **liwc** experiments, except when the correlation has been computed exactly around the pseudo-observation track for the period between t+9 and t+6-hour forecasts (period closest to the pseudo-observation usage in 4D-Var). Except for the first 3-hour accumulated period, all **refl** experiments have larger correlations than the **ref** run.

To show where modifications to the precipitation fields are mainly happening in the forecast, 12-hour accumulated precipitation (between 24 April 2008 12:00 UTC and 25 April 2008 00:00 UTC) from NEXRAD precipitation data and from the forecast starting from the reference assimilation system and from analyses created by the different 4D-Var experiments is displayed in Fig. 4.10. The reference run has a precipitating region more widely spread than indicated by observations and also the south end of intensive precipitation (around 10 to 15 mm h^{-1} according to the NEXRAD observations) on the east side of precipitation pattern is localized further north (above 40°N). Precipitation intensity over Lake Superior is smaller. All experimental runs are trying to narrow the whole precipitation region and to intensify precipitation over the lake. Experiments **refl2err** and **refl1.5err** also move the high precipitation band on the west side of the precipitation area (north of 45°N) present in the reference run east of 95°W longitude which is more consistent with the NEXRAD data hardly giving any precipitation there. One can notice that both **liwc** and **liwc2err** experiments are good at reducing precipitation on the edges or even starting to create a hook-shaped feature south of the Lake Michigan. However, they are less successful in modifying the central precipitation region. Table 4.2 also confirms the worse performance of **liwc** and **liwc2err** experiments compared to the **ref** run. On the other hand, reflectivity experiments correctly try to intensify and/or reduce the precipitation amount over several areas which lead to better spatial correlations, especially for **refl2err** and **refl1.5err**.

The verification of the impact of 1D+4D-Var CloudSat data assimilation on cloud forecasts has been carried out through a comparison to infrared geostationary imagery (10.7 μm) from the GOES-12 satellite, which represents another independent source of validation data. Simulated images have been computed from the ECWFW model temperature, moisture, cloud and ozone fields using the RTTOV-9 radiance transfer model

(http://research.metoffice.gov.uk/research/intreproj/nwpsaf/ rtm/rtm_rttov9.html) to perform the validation in 10.7 μm brightness temperature space. Figure 4.11 shows the impact of assimilating T and q pseudo-observations on simulated TBs from the 9-hour long forecast (starting at 12:00 UTC) compared to GOES-12 observations. Impact is computed in the same way as for precipitation (see above). 19:00 UTC is the closest time to the time slot in which the pseudo-observations were used in the assimilation system. The results are only shown for one of the experiments, **refl2err**, which showed improved correlation with observed precipitation data. Mean impact computed over the whole domain shown on the figure would be slightly negative for the experimental run when compared against GOES TBs and slightly positive when compared against the NEXRAD precipitation data. However, when concentrating on the area just around the CloudSat satellite track, positive local impact on TBs can be found. Larger positive impact (marked by black ovals in Fig. 4.11) is mostly outside of the observed precipitation zone, south of 40°N (Fig. 4.11c). In the precipitating area, the positive impact on TBs (marked by green ovals) is very small around the track, but it corresponds well to precipitation improvement (Fig. 4.11d). This correspondence between precipitation and TBs improvement is also true for off-track pattern in the middle of 40°N-50°N and 100°W-90°W area.

In addition to the improvements in the precipitation pattern in Fig. 4.9, 4.10c-e and Table 4.2, the changes in the rms wind errors at 200 hPa are depicted in Fig. 4.12 (shown for **refl2err** experiment only). Wind and precipitation errors are strongly related through the diabatic heating and the associated vertical mass flux with upper-level divergence. Wind improvement, especially at levels around 200 hPa, has already been indicated by results from the verification of the assimilation runs against other assimilated observation types for the domain over the Eastern USA (Fig. 4.8). Figure 4.12 shows how the signal of reduced, resp. increased rms errors from the experimental run propagates in time up to 48-hour forecast. Generally, rms errors are mostly reduced in **refl2err** experiment, which is also demonstrated in Table 4.3 providing rms errors over the domain displayed in Fig. 4.12. Furthermore, the impact on 200 hPa winds from pseudo-observations (temperature mainly) is long-lived and propagates far away from observations. This indicates a potential benefit from the assimilation of cloud information in a 4D-Var system, through the link with the dynamics.

Period	0 - 3	3 - 6	6 - 9		9 - 12	0 - 12
EXP				Domain B		
ref	0.602	0.583	0.510	0.689	0.460	0.613
refl	0.551	0.585	0.531	0.705	0.454	0.614
refl2err	0.586	0.597	0.526	0.718	0.482	0.618
refl1.5err	0.610	0.619	0.538	0.741	0.496	0.646
liwc	0.605	0.532	0.485	0.712	0.398	0.565
liwc2err	0.578	0.604	0.497	0.704	0.302	0.579

Table 4.2: *Statistics of precipitation accumulations for the forecast periods (in hours) as described in the table header from the reference run* **ref** *and from the different assimilation experiments (see text for experiment description) versus NEXRAD precipitation data for the case of 24 April 2008 over the USA. Correlation coefficients are computed for all indicated time periods over domain A (30°N-51°N and 100°W-85°W) and for the period between t+9 and t+6-hour forecasts also over the smaller domain B (30°N-51°N and 94°W-87°W) as displayed on Fig. 4.9.*

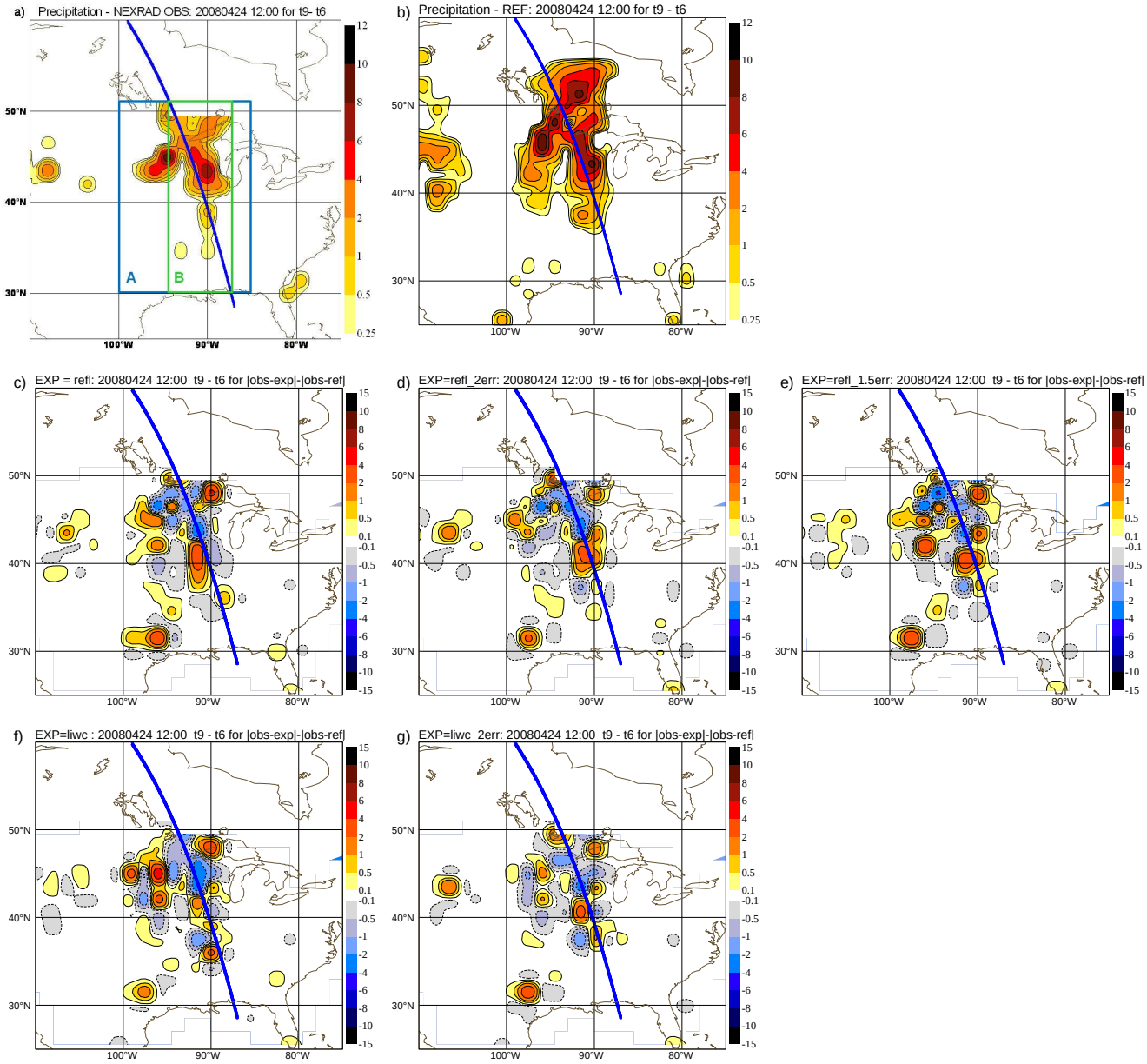

Figure 4.9: *Impact (expressed as* $\overline{|obs-exp|-|obs-ref|}$*) on 3-hour accumulated precipitation between t+9- and t+6-hour forecasts starting from analyses on 24 April 2008 at 12:00 UTC created by the different 4D-Var experiments (exp) assimilating T and q pseudo-observations retrieved from 1D-Var of cloud radar reflectivity (c-e) or cloud liquid and ice water contents (f-g) using observation errors as derived from the 1D-Var analysis covariance matrix (c,f), twice as large (d,g) and 1.5 times as large (e) as the computed ones. 3-hour accumulated precipitation (mm* h^{-1}*) are shown for the observations (obs) - NEXRAD precipitation data (a) and for the reference (ref) run (b), i.e. without pseudo-observation assimilation. Rectangles in panel (a) indicate the domains for which the statistics in Table 4.2 have been computed. Blue line represents the CloudSat track.*

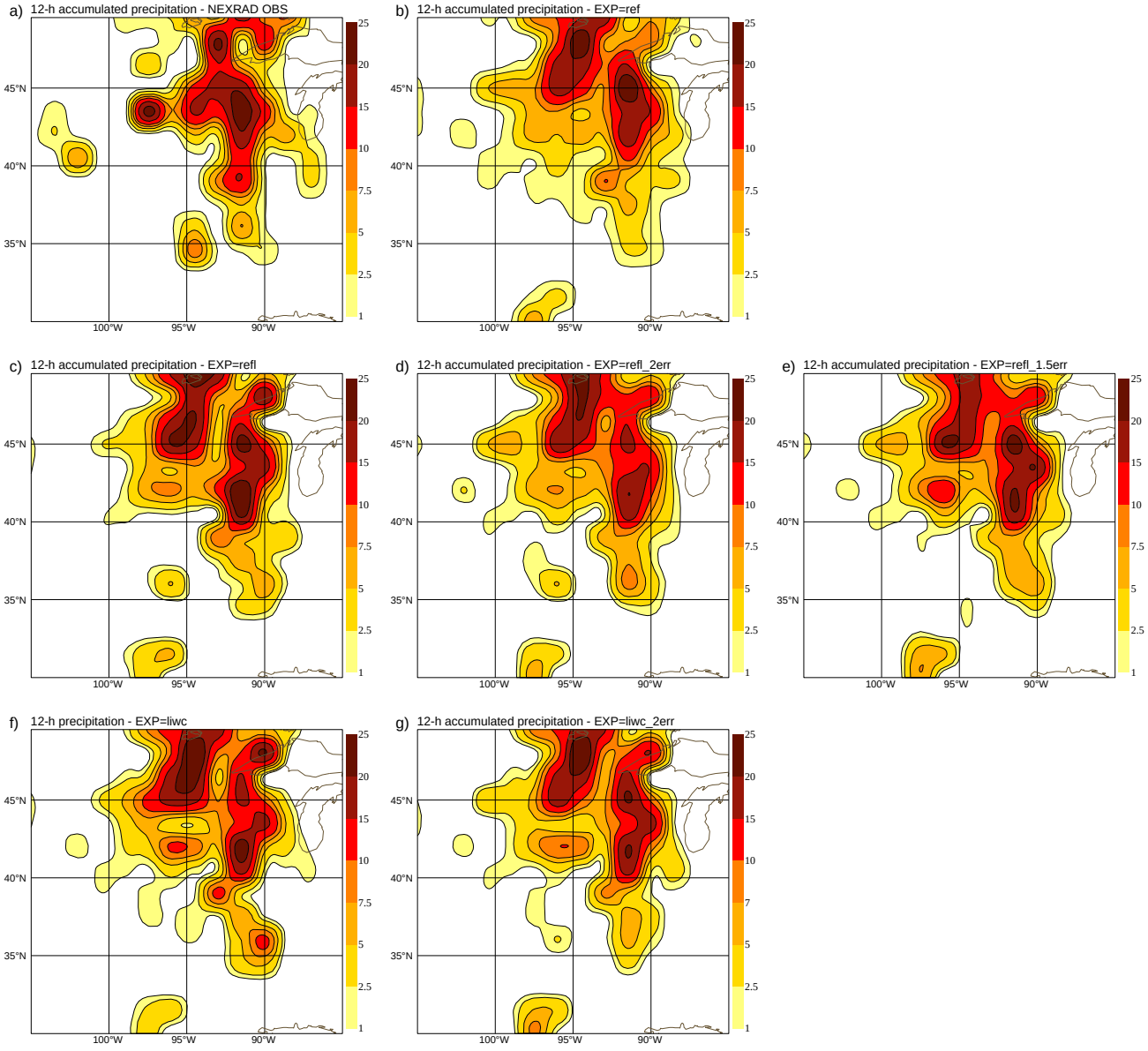

Figure 4.10: *12-hour accumulated precipitation (between 24 April 2008 12:00 UTC and 25 April 2008 00:00 UTC) from NEXRAD precipitation data (a), from the forecast starting from the reference assimilation system (b) and from the forecasts starting from analyses created by the different 4D-Var experiments assimilating T and q pseudo-observations retrieved from 1D-Var with cloud radar reflectivity (c-e) or cloud liquid and ice water contents (f,g) using observation errors as derived from the 1D-Var analysis covariance matrix (c,f), twice as large (d,g) and 1.5 times as large (e) as the computed ones.*

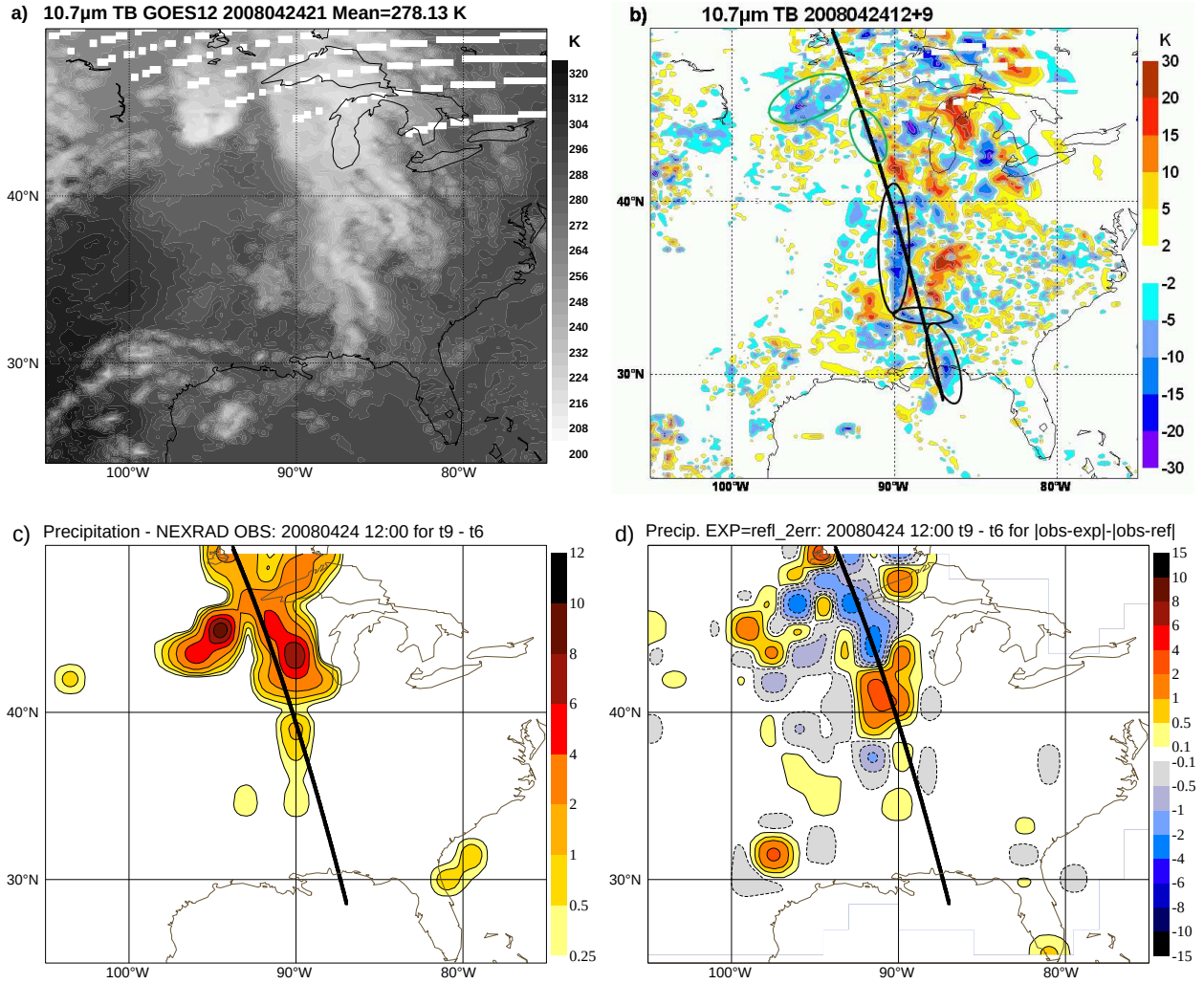

Figure 4.11: *Impact of assimilating T and q pseudo-observations retrieved from 1D-Var of cloud radar reflectivity using observation errors twice as large as the computed ones on 10.7 µm simulated TBs from 9-hour forecast compared to GOES-12 observations (b) and on 3-hour accumulated precipitation between t+6- and t+9-hour forecasts (d) starting on 24 April 2008 at 12:00 UTC. (a) displays 10.7 µm simulated TBs (in K) on the same day at 21:00 UTC and (c) 3-hour accumulated NEXRAD precipitation (in mm h^{-1}) between 19:00 and 21:00 UTC. Positive (resp. negative) impact is shown with blue (resp. red) shadings.*

FC length [h]	12	24	36	48
EXP				
ref	1.304	2.025	2.510	3.438
refl2err	1.259	1.978	2.416	3.361

Table 4.3: *Rms errors for the differences: (**ref**) between the forecast starting from the reference analysis and corresponding reference analysis and (**refl2err**) between the forecasts starting from the experimental assimilation and the reference analysis. Statistics is computed for 12-, 24-, 36- and 48-hour forecasts over domain displayed in Fig. 4.12.*

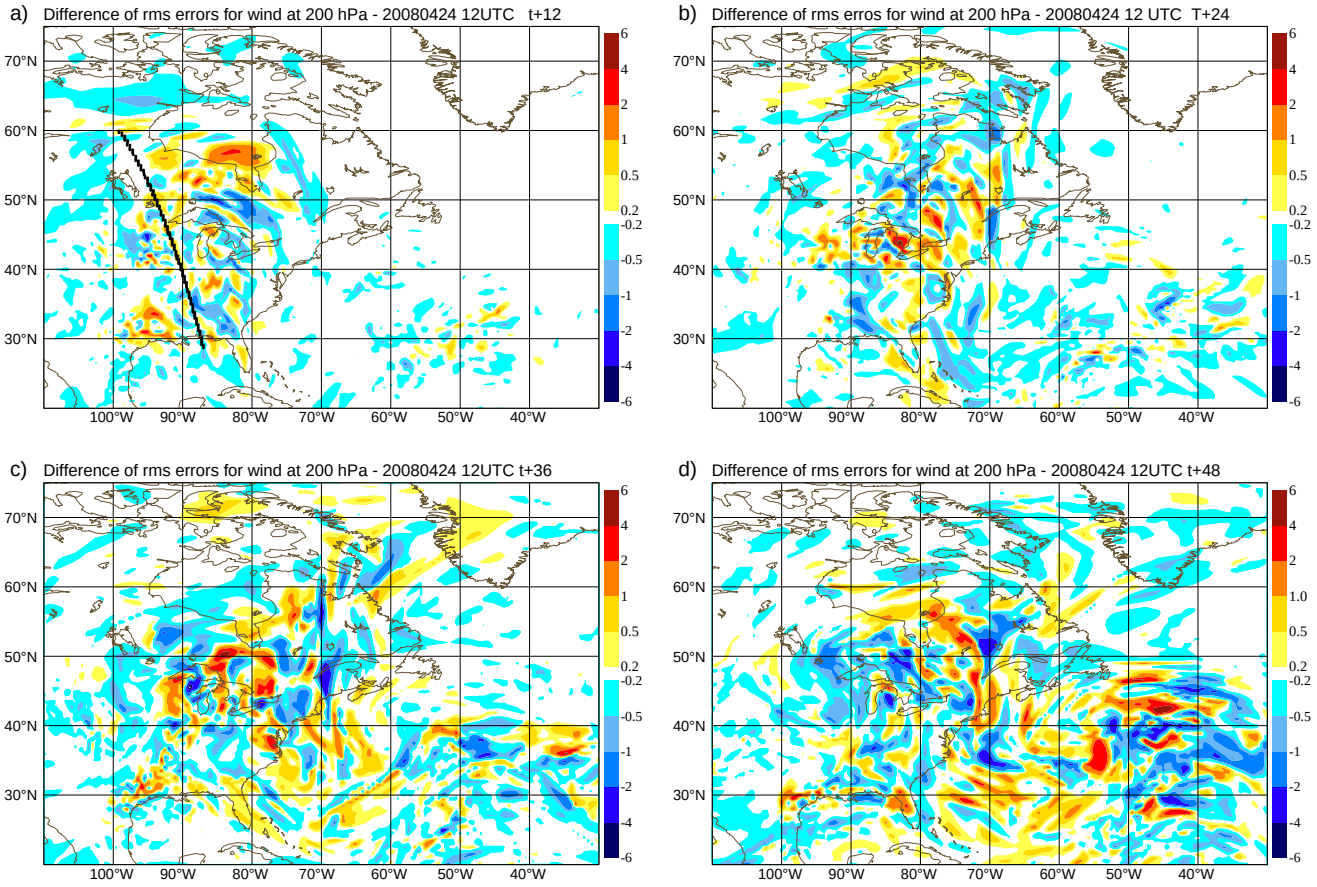

Figure 4.12: *Difference of 200-hPa wind rms errors for the differences between the forecasts starting from analysis created by 4D-Var assimilation of T and q pseudo-observations retrieved from 1D-Var with cloud radar reflectivity using observation errors twice as large as the computed ones from the 1D-Var analysis covariance matrix and the reference analysis and between the forecasts starting from the reference analysis and corresponding reference analysis. (a) 12-hour, (b) 24-hour, (c) 36-hour and (d) 48-hour forecasts. Reduction (resp. increase) of rms errors for the experimental run is shown with blue (resp. red) shadings.*

4.3.2 *Situation on 16 September 2007 - tropical cyclone*

Typhoon Wipha originated from a tropical disturbance on 15 September 2007. Wipha quickly developed into a tropical storm as deep convection formed around the centre of circulation. The following day, the system rapidly intensified into a typhoon and continued to become increasingly organized. Wipha reached its peak intensity on 18 September 2007 with winds of 185 km h^{-1} and with a minimum pressure of 925 hPa. On 16 September 2007 00 UTC (date of our assimilation experiments), Wipha was a tropical storm with a central pressure of 992 hPa. As mentioned in WP-3100, this is a more challenging situation since the first-guess departures are more significant in this case.

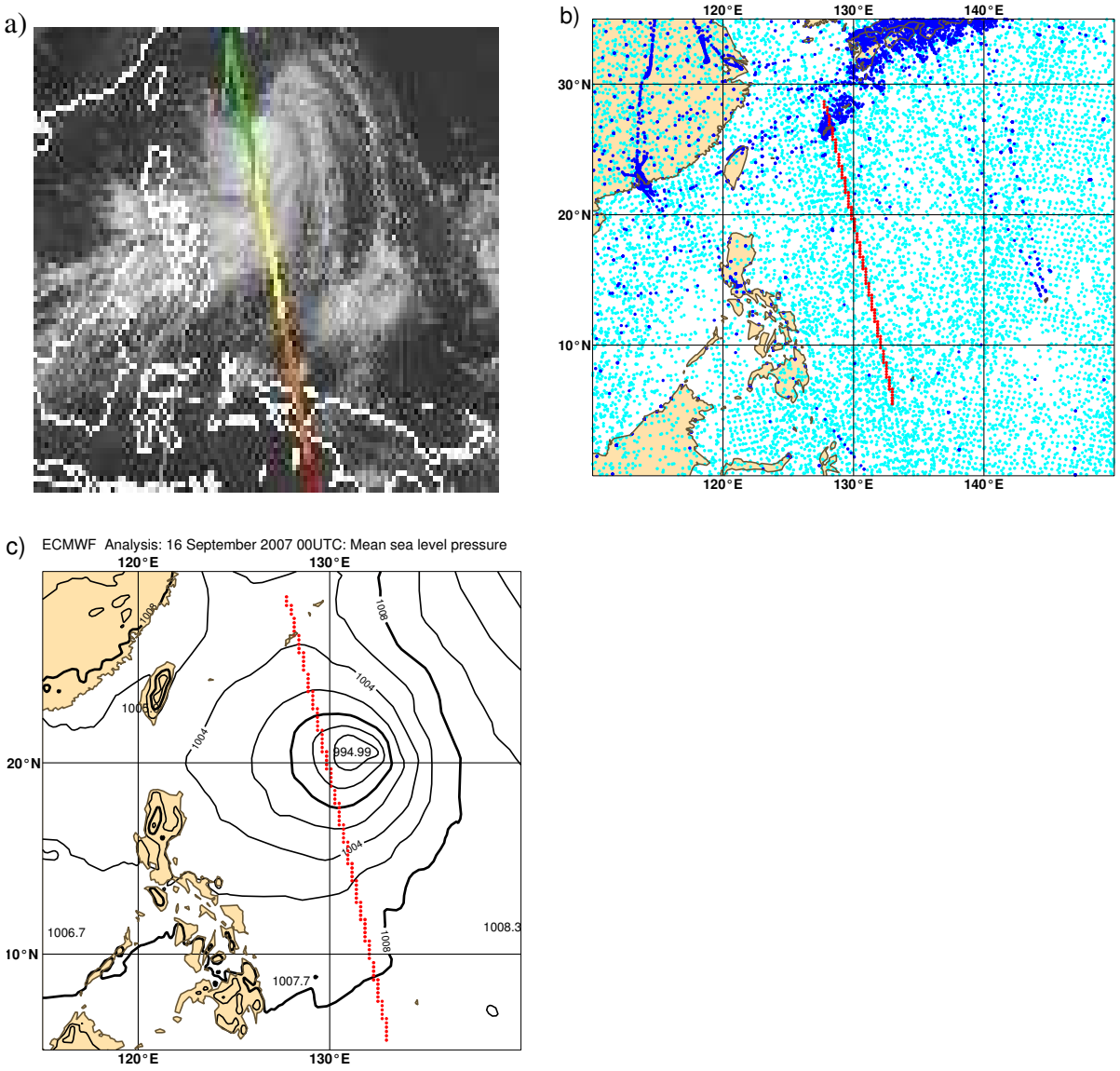

Figure 4.13: *Satellite infrared image of tropical cyclone Wipha on 16 September 2007 at 4:00 UTC (a) and data coverage over the area used in 4D-Var assimilation system (b): conventional observations (dark blue), satellite observations (cyan) and pseudo-observations from 1D-Var with CloudSat observations (red). Mean sea level pressure from reference analysis (c).*

The satellite track for the situation on 16 September 2007 between 4:48 and 4:54 UTC is displayed in Fig. 4.13. It crosses over a tropical cyclone in the west Pacific and it is covered by 123 model grid points. It also shows observational data coverage over the domain in the vicinity of the CloudSat satellite track. As for the

case over the USA, there is a large amount of standard observations, in this case mostly satellite ones, which were used by the 4D-Var system.

Results from different assimilation experiments (described in subsection 4.1) are provided in Fig. 4.14 - 4.20 and in Table 4.4.

(a) Comparisons of the first-guess and analysis against assimilated observations

Probability distribution functions (PDF) of the first-guess and the analysis departures for the pseudo-observations are shown in Fig. 4.14 (for temperature) and Fig. 4.15 (for specific humidity). While the PDFs of the first-guess departures for temperature are very similar whether the T and q pseudo-observations are coming from 1D-Var of cloud radar reflectivity or cloud liquid and ice water contents, PDFs of specific humidity for experiments assimilating cloud liquid and ice water contents have a noticeable tail for negative departures (i.e. when model is moister than pseudo-observations). This is due to the fact that the model FG system is more widely spread and has more continuous cloud cover on the northern and especially on southern edges of the storm system, compared to CloudSat observations. The 1D-Var assimilation of cloud liquid and ice water contents was very efficient in removing this excessive cloud cover, much more than the assimilation of cloud reflectivity. It seems that this larger cloud reduction, consistent with the CloudSat observations, required a larger reduction in specific humidity, thus creating a tail in the PDF of first-guess departures for specific humidity. When looking at the analysis departures, it is more obvious here than for the case of 24 February 2008 that using larger errors for the pseudo-observations leads to more narrow PDFs of the analysis departures for the reasons explained in subsection 4.3.1 *(a)*. Actually, when using the observation errors as retrieved from the 1D-Var analysis covariance matrix, AN departures for temperature hardly changed compared to FG departures. For specific humidity, some narrowing of the AN departures is noticeable, though it is larger when using inflated observation errors. Table 4.4 containing bias and standard deviation (stdv) of the first-guess and analysis departures for the different assimilation experiments shows that also standard deviations are smaller for the experiments with larger pseudo-observation errors. Generally, according to the table, standard deviation of the AN departures for all experiments is reduced with respect to FG departures, even for temperature and from experiments with non-inflated observation errors.

Figures 4.16 (for temperature) and 4.17 (for specific humidity) show two-dimensional PDFs of analysis-minus-observation versus background-minus-observation. This diagnostics provides a more detailed picture about the performance of the different assimilation experiments. The round shape of 2D PDFs for temperature when using observation errors computed from Eq. 3.1 clearly shows that AN departures have hardly been modified. When using the double observation errors, the analysis departures are reduced. In the case of specific humidity, better performance is again obtained for the experiments with large observation errors. For both **refl2err** and **liwc2err**, the system is better at reducing than at increasing specific humidity.

PDF diagnostics, similarly as in the case of 24 February 2008, show that using observation errors comparable to other T and q observations reduces the analysis departures more than trying to constrain the 4D-Var towards one type of observations only. This indicates that appropriate weight given to the new observations should be carefully considered through the suitable definition of observation errors.

Profiles of T and q bias and standard deviation for the first-guess and analysis departures from the different 4D-Var experiments are shown in Fig. 4.18 and 4.19 providing information about the vertical structure of the model departures from assimilated observations. As in the previous case, the vertical profiles of temperature standard deviation for the FG departures are extremely similar for the pseudo-observations coming either from 1D-Var with cloud radar reflectivity or cloud and ice water contents. There is just small difference in bias in the levels below 900 hPa. Differences in the FG departures are more substantial for specific humidity, especially for the bias profiles. This is consistent with PDFs of the first-guess departures. For this cyclone case, it is obvious also from the vertical distribution that experiments with larger observation errors have

smaller AN departures for T (**refl2err**, **liwc2err**) and q (**liwc2err** mainly).

The assimilation runs have also been verified against other assimilated observation types for the domain over tropical cyclone as shown in Fig. 4.13. Generally, no significant changes have appeared when considering observations-minus-background and observation-minus-analysis departures statistics (not shown) for all types of observations assimilated in 4D-Var and over the selected domain. This again proves that it is difficult to improve the fit to other observations by including new ones over a domain well covered by a large amount of measurements.

(b) Impact of 1D+4D-Var assimilation on the subsequent forecast

An evaluation of the skill of the 1D+4D-Var system for assimilation of the cloud radar observations and impact of this assimilation on the subsequent forecast is done by comparing the forecast track with observed track data for tropical cyclone Wipha. The model tracking algorithm locates the cyclone by determining the position of the minimum mean-sea-level pressure and maximum vorticity via a recursive search mechanism (van der Grijn, 2002). A modification of the temperature and the specific humidity fields during the 4D-Var assimilation which takes into account the temporal evolution of any variable within the assimilation window can trigger a dynamical response in the model. This can lead to a better location of the cyclone at the analysis time and it also could generate (in ideal conditions) a better forecast of the cyclone itself in terms of both location and intensity.

Figure 4.20 shows a comparison of the observed track with the forecast track from the reference run and from four 1D+4D-Var experiments of the cloud radar observations (**refl**, **refl2err**, **liwc**, **liwc2err** - described in section 4.1). The cyclone track was quite well forecast by the reference run beyond the first 12 hours after analysis, however the cyclone at the analysis time was misplaced, being more than 0.6° (i.e. 67 km) to the north from the observed position. Note that the symbols for different experiments are shown at each 6 hours for the first 12 hours of the forecast (starting from 0, i.e analysis time) and then every 12 hours. These symbols indicate the cyclone position at the corresponding times for the different experiments. The assimilation of cloud radar data generally improves the initial position of the cyclone. It is nearly spot on at the observed location for the **liwc** and **liwc2err** experiments. For the **refl** experiments, the cyclone is in comparable distance from the observed track as in the reference run already for 6-hour forecast. However, for the **liwc** experiments (especially **liwc2err**) the forecast track is closer to the observed one up to 12 hours. The mean-sea-level pressure along the cyclone track is very similar for all runs (reference and experimental ones). After the first 12 hours of the forecast, however, the better the cyclone was positioned in the analysis, the worse the track would become in the longer forecast. This underlines how chaotic the system can be in the case of such an event as a tropical cyclone. Even providing better initial conditions does not necessary lead to a better cyclone track in longer forecasts. In this studied case, cloud radar data indicated a good potential for analysis and only very short-range forecast improvements.

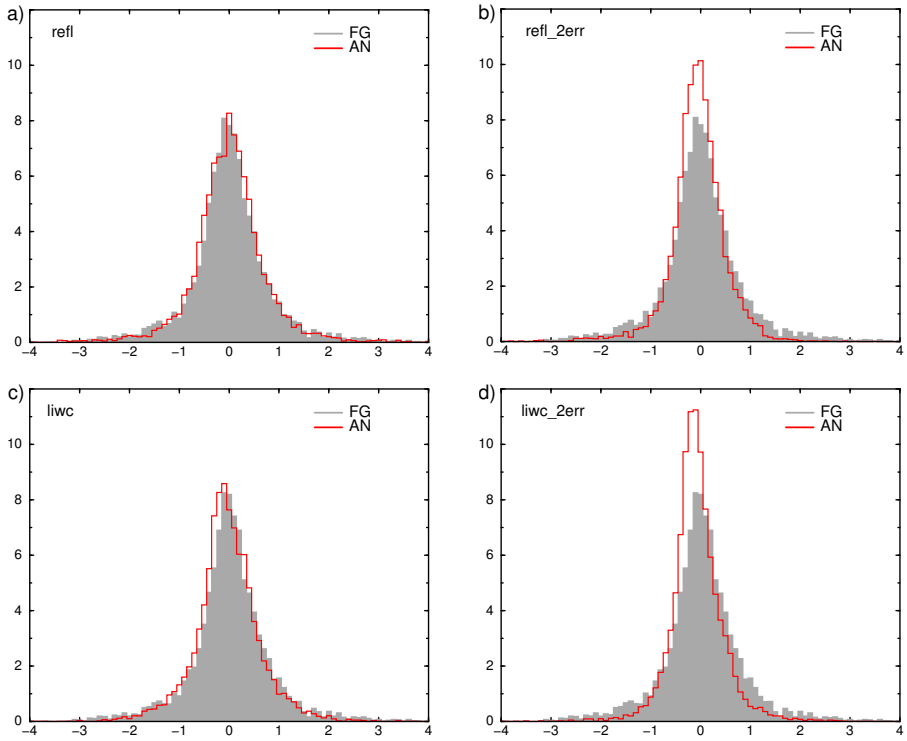

Figure 4.14: *Probability distribution function (PDF) of first-guess (grey shading) and analysis (red line) departures for temperature (K) when pseudo-observations were retrieved from 1D-Var with cloud radar reflectivity (a,b) or cloud liquid and ice water contents (c,d) using observation errors as derived from the 1D-Var analysis covariance matrix (a,c) and two times larger (b,d) than the computed ones. Case of 16 September 2007.*

	T		q	
	bias	stdv	bias	stdv
FG-refl	0.027	0.866	-0.1079	0.8288
AN-refl	0.004	0.766	0.0049	0.7751
AN-rel2err	-0.064	0.588	-0.0149	0.7562
FG-liwc	-0.039	0.865	-0.4766	1.0435
AN-liwc	-0.042	0.709	0.0069	0.6720
AN-liwc2err	-0.087	0.602	-0.0527	0.5716

Table 4.4: *Bias and standard deviation (stdv) of the first-guess (FG) and analysis (AN) departures for the different assimilation experiments (see text for experiment description). FG-refl departures are for the experiment when pseudo-observations were retrieved from 1D-Var with cloud radar reflectivity and FG-liwc when retrieved from 1D-Var with cloud liquid and ice water contents. 123 profiles were included in the statistics for the case of 16 September 2007.*

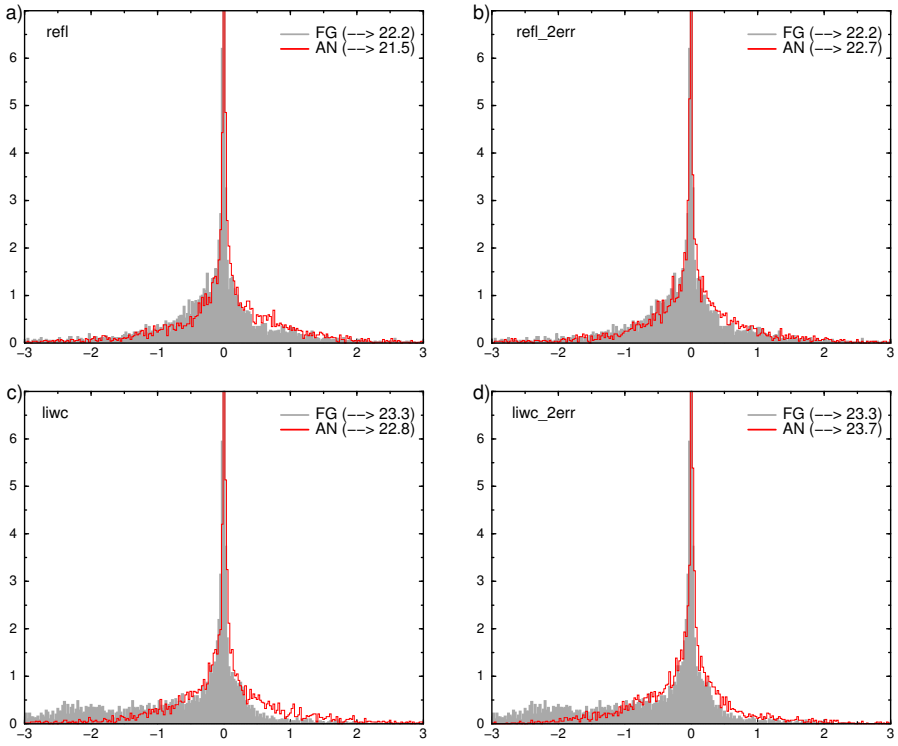

Figure 4.15: *Same as Fig. 4.14, but for specific humidity (g kg^{-1}).*

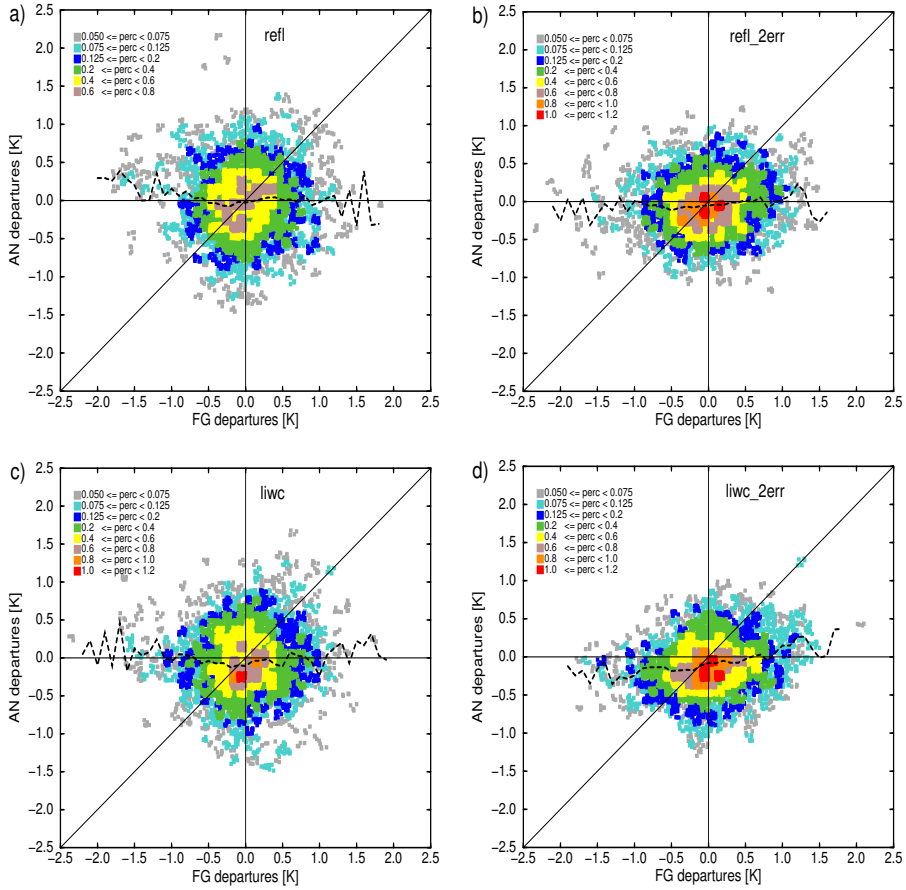

Figure 4.16: *2D PDF of analysis-minus-observation versus background-minus-observation departures for temperature (K) from different 4D-Var experiments assimilating T and q pseudo-observations retrieved from 1D-Var with cloud radar reflectivity (a,b) or cloud liquid and ice water contents (c,d) using observation errors as derived from the 1D-Var analysis covariance matrix (a,c), twice as large (b,d) as the computed ones. Colour shading indicates frequency in % while the black dashed line corresponds to the mode of the analysis departure distribution for each background departure class. Case of 16 September 2007.*

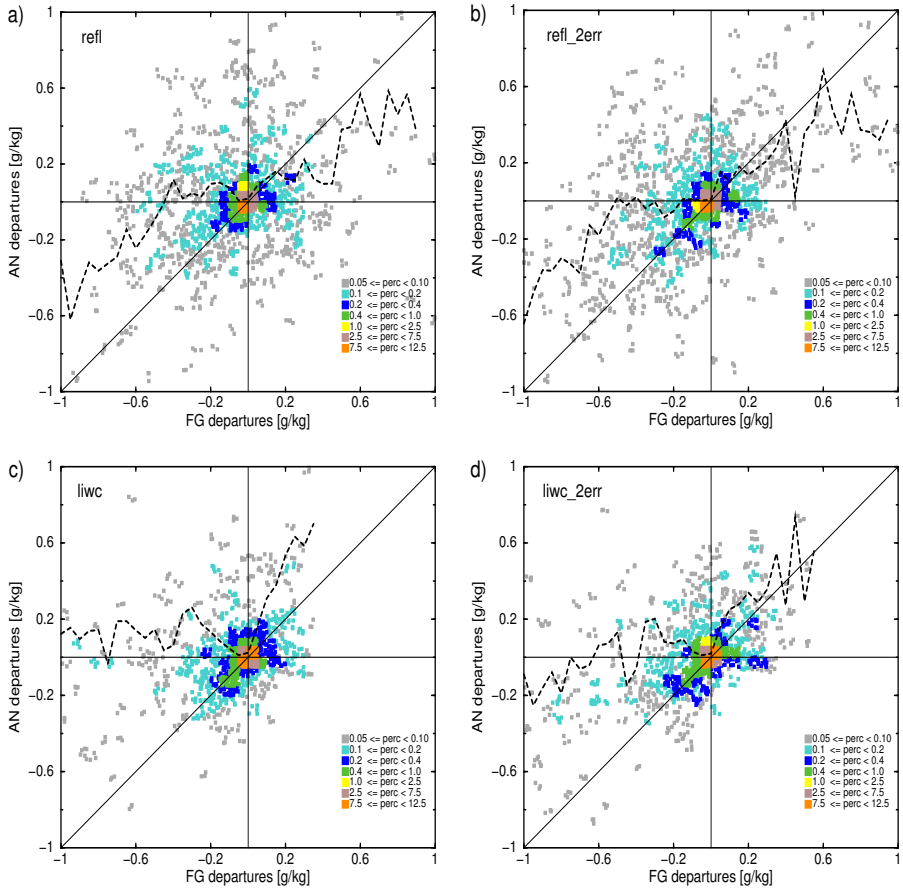

Figure 4.17: *Same as Fig. 4.16, but for specific humidity (g kg^{-1}).*

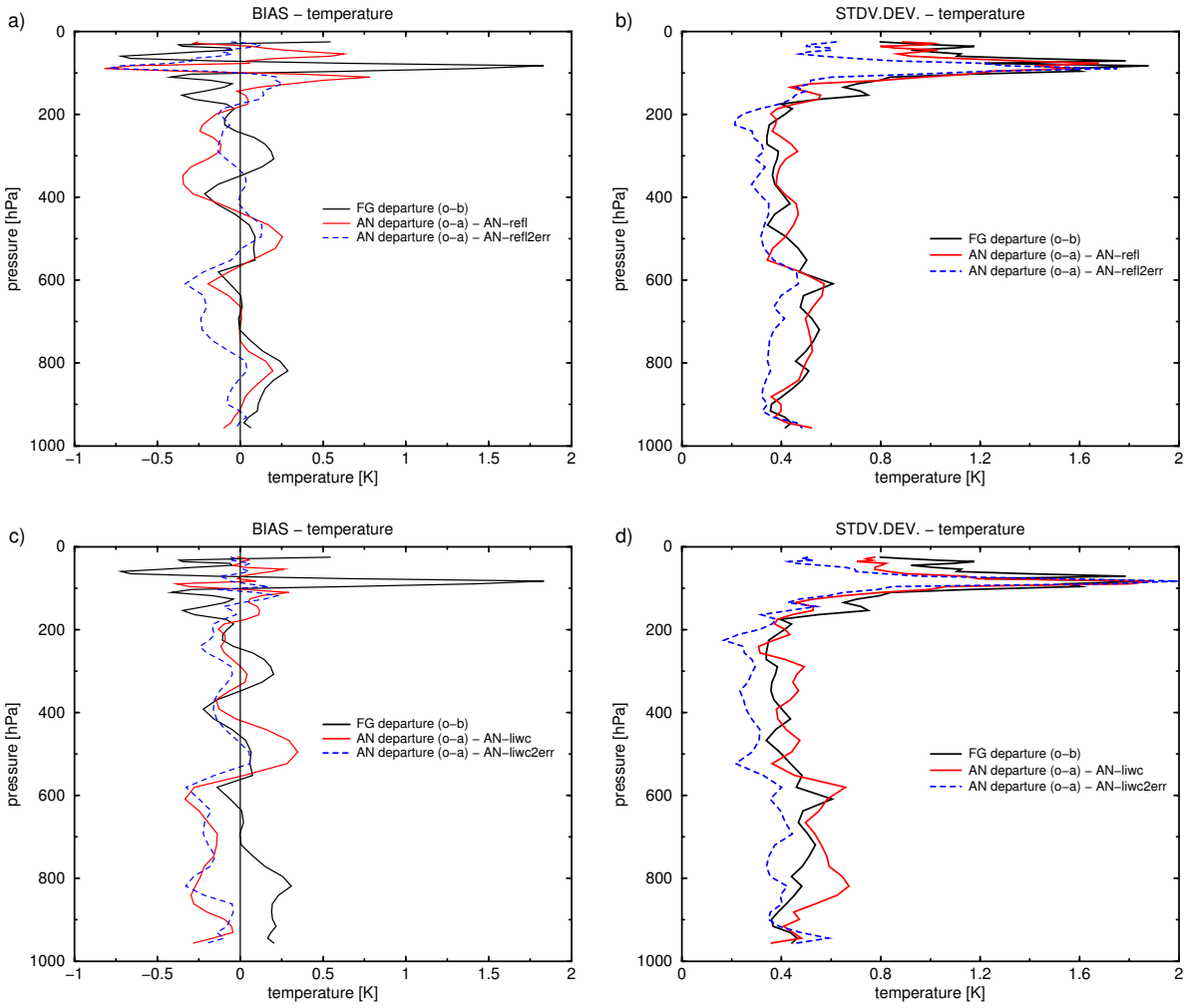

Figure 4.18: *Profiles of temperature (in K) bias (a,c) and standard deviation (b,d) for the first guess (black solid line) and analysis departures (different colour lines as explained by figure legends) from different 4D-Var experiments assimilating pseudo-observations retrieved from 1D-Var of cloud radar reflectivity (top) or cloud liquid and ice water contents (bottom). Case of 16 September 2007.*

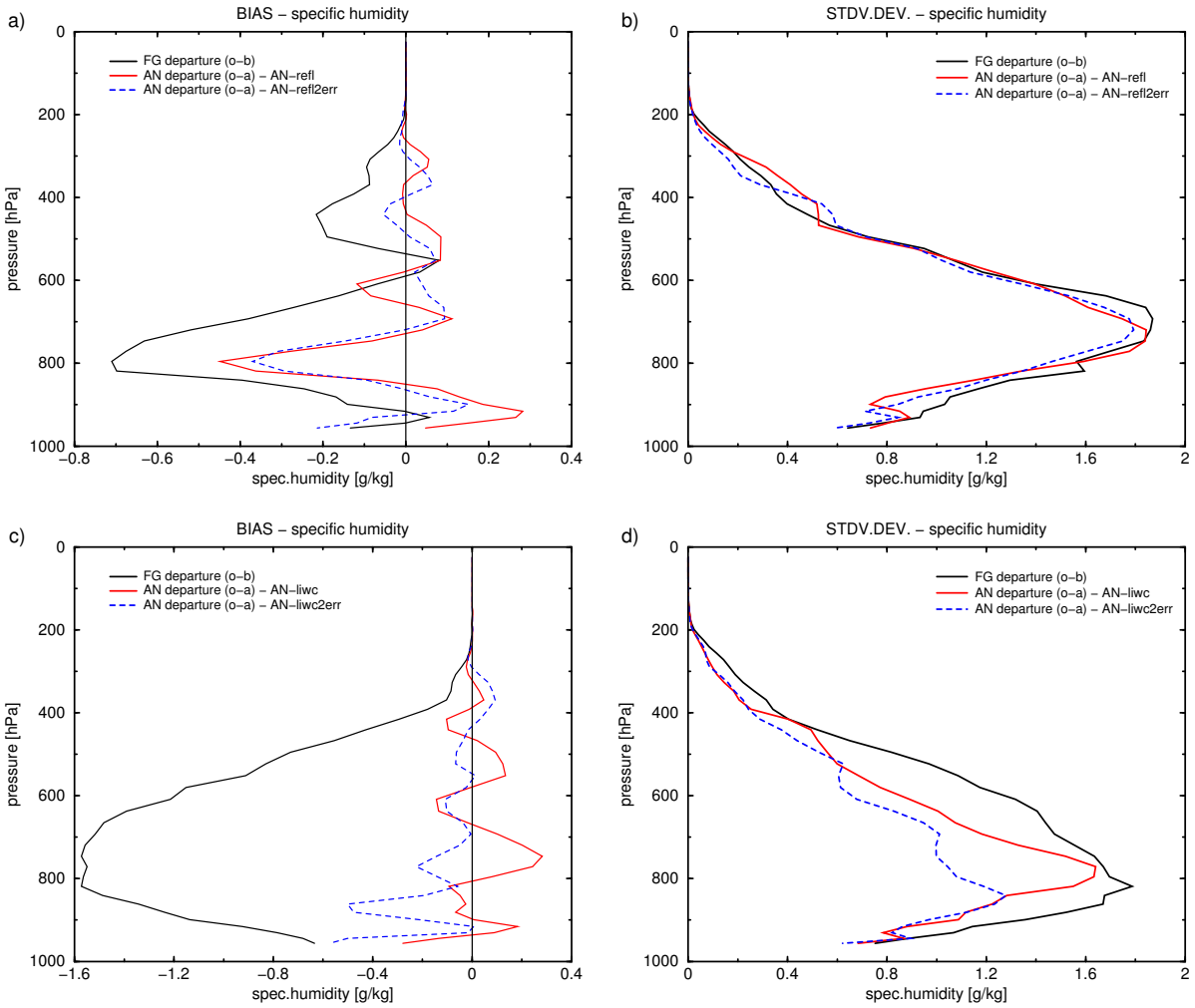

Figure 4.19: *Same as Fig. 4.18, but for specific humidity (g kg^{-1}).*

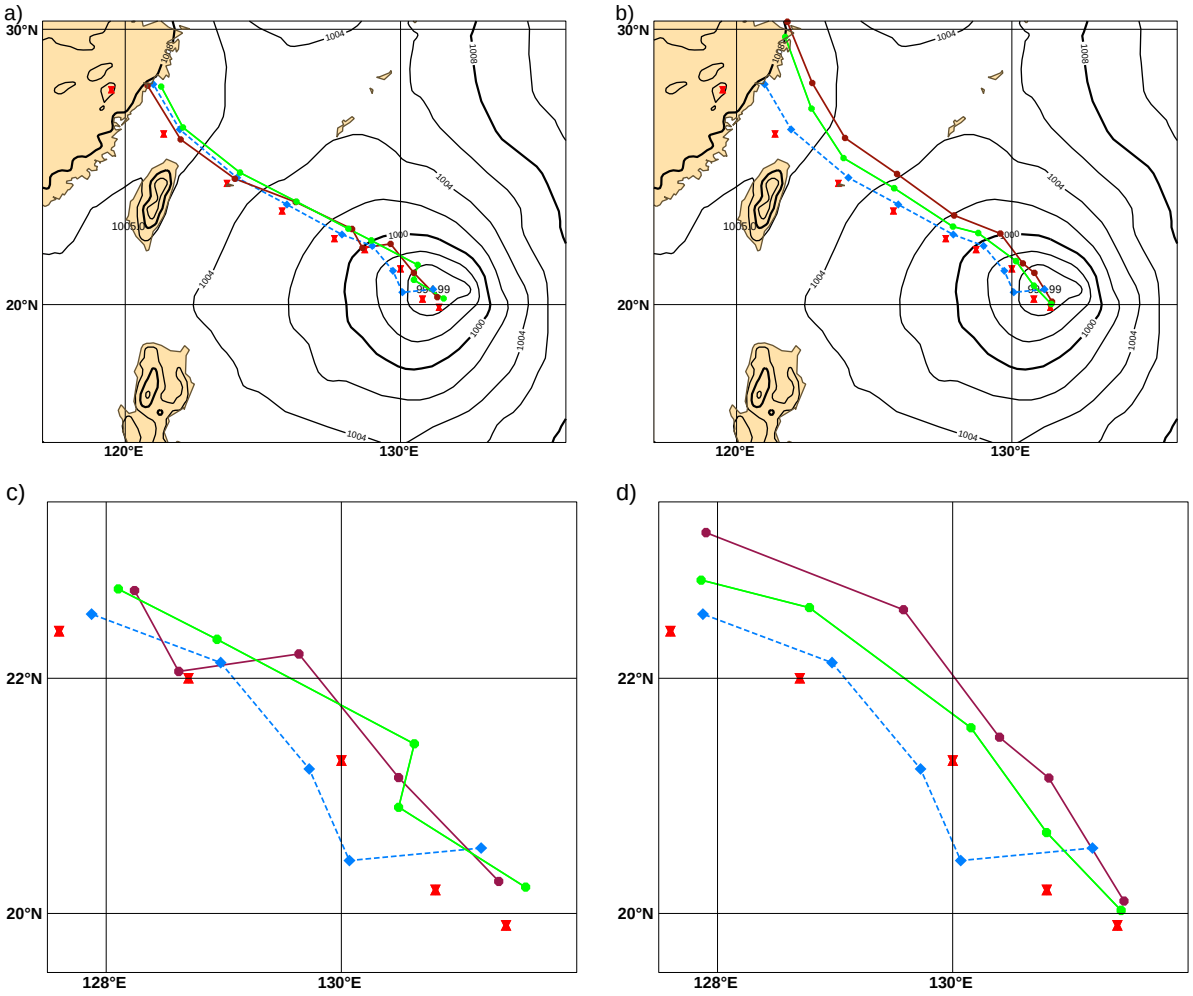

Figure 4.20: *Comparison of forecast tracks with observed track of tropical cyclone Wipha on 16 September 2007: observations (red marks), control run (blue dashed line), 4D-Var experiments assimilating T and q pseudo-observations retrieved from 1D-Var using observation errors as derived from the 1D-Var analysis covariance matrix (brown solid lines) and errors two times larger than computed ones (green solid lines). Results from the assimilation of pseudo-observations retrieved from 1D-Var with cloud radar reflectivity are shown on left panels (a,c) and from 1D-Var with cloud liquid and ice water contents on right panels (b,d). (c), resp. (d) is zoom over the cyclone tracks displayed on (a), resp. (b) where mean sea level pressure from reference analysis on 16 September 2007 00:00UTC is also displayed.*

5 Conclusion and perspectives

In this work package, feasibility studies have been performed in order to study the impact of cloud observations from active sensors on 4D-Var analyses and subsequent forecasts. A 1D+4D-Var technique has been selected for this purpose since this approach is more easily applicable to the new observation types and since it was also originally used operationally at ECMWF to assimilate rain rates or rain affected radiances. In this two-step strategy, a 1D-Var assimilation technique is first used to assimilate either CloudSat reflectivities (level-1 products) or retrieved cloud liquid and ice water contents (level-2 products). This creates profiles of specific humidity and temperature, which are then included as pseudo-observations in the 4D-Var system. Since T and q pseudo-observations come from the 1D-Var retrievals, their observation errors correspond to the 1D-Var retrieval errors. Therefore these errors have been derived from the 1D-Var analysis error covariance matrix. They appeared to be on average approximately twice as small as errors used for instance for the radiosonde temperature and specific humidity measurements. Since observation errors influence the impact of observations in data assimilation, experiments have also been performed with increased errors compared to those which were computed initially.

Several 4D-Var experiments have been run for a couple of selected meteorological situations and an evaluation of the obtained analysis and the subsequent forecasts (mainly short range) has been done. This experimentation should be considered as a feasibility study investigating the possibility of using new observations and their potential impact in the NWP system. It does not allow to draw any firm conclusions yet about the usefulness of the data in an operational context. That would require to run experiments over several months and therefore further significant model developments to perform a proper assimilation cycling. Given the length of this project and time which was assigned to this work package, only experimental studies for a few cases could be performed. Nevertheless, they already provide some indications about their potential impact.

The results from the 1D+4D-Var experiments have shown that information on specific humidity and temperature retrieved from 1D-Var of cloud radar data and assimilated as pseudo-observations into the 4D-Var system can lead to improved initial conditions and partially better forecast for the selected cases. When comparing the first-guess and analysis departures for the pseudo-observations, it has been observed that experiments with larger observation errors (i.e. errors comparable to other T and q observations) reduce the analysis departures further. Also the subsequent forecast seemed to be improved in that case. This indicates that appropriate weight given to the new observations should be investigated through a suitable definition of the observation errors. To compute errors from the 1D-Var analysis error covariance matrix is quite expensive for profiling observations and only affordable for non-operational applications. A statistical approach should rather be used for the definition of errors. This raises the question whether it would not be more suitable to use a direct 4D-Var assimilation of cloud radar data, which would only require the proper definition of observation errors for reflectivities or cloud liquid and ice water contents (which are anyhow needed even in the 1D-Var system).

The assimilation runs have also been verified against other observation types assimilated in 4D-Var. No significant changes have been observed in observation-minus-background and observation-minus-analysis departure statistics for these observations. This indicates that it is not easy to achieve a significant improvement in the fit to other observations by including the new ones over a domain over which a lot of other measurements are already assimilated. To get more impact from the new data would require to carefully tune their usage in the assimilation system.

When studying the impact of new observations on the subsequent forecast, some improvement in the precipitation forecast has been found in some assimilation experiments. Since wind and precipitation errors are related through the diabatic heating and the associated vertical mass flux with upper-level divergence, a wind improvement at 200 hPa has also been noticed for those experiments. This impact on 200 hPa winds from

pseudo-observations seemed to be long-lived and to propagate far away from observations. This suggests a potential benefit from assimilating cloud information through the link with the dynamics in the 4D-Var system. Comparisons of the observed tropical cyclone track with the forecast track revealed that the assimilation of cloud radar data is able to improve the initial position of the cyclone, but this improvement may only be short-lived in the forecast due to chaotic nature of tropical cyclones.

The performed feasibility study provides some hints what one could expect from assimilating cloud information from active sensors. Real assimilation of such measurements would still require a substantial amount of work to fully benefit from these observations. Some of the necessary improvements were already suggested by 1D-Var experiments, such as building a suitable bias correction for these cloud observations or re-testing the reflectivity observation operator for non-linearities, which can have a negative impact on assimilation performance. Another issue which should be considered is better screening of observations. Improved observation error definition (including representativeness error) is also required.

Acknowledgements

Special thanks belong to my colleague Philippe Lopez for fruitful discussions and helpful advices, as well as for providing verification using GOES data. I am also grateful to Fernando Prates for preparing the cyclone tracking and Angela Benedetti for discussions and suggestions preparing this manuscript. I would further like to thank Peter Bauer and Anton Beljaars for proof reading and their constructive comments on the manuscript. The NASA CloudSat Project is kindly acknowledged for providing the CloudSat data. The Stage IV precipitation observations were produced by NCEP and provided by JOSS/UCAR. NOAA should be acknowledged for supplying GOES-12 satellite data through CLASS.

A List of Acronyms

1D-/4D-Var	One-/Four-Dimensional Variational assimilation
AN	analysis
AIREP	aircraft weather reports
CALIPSO	Cloud-Aerosol Lidar and Infrared Pathfinder Satellite Observation
CLASS	Comprehensive Large Array-data Stewardship System
CloudSat	NASA's cloud radar mission
EarthCARE	Earth, Clouds, Aerosols and Radiation Explorer
ECMWF	European Centre for Medium Range Weather Forecasts
FG	first guess
GES DISC	Goddard Earth Sciences Data and Information Services Center
GOES	Geostationary Operations Environmental Satellite
IFS	Integrated Forecast System
JOSS/UCAR	Joint Office for Science Support of the University Corporation for Atmospheric Research
MODIS	Moderate Resolution Imaging Spectroradiometer
NASA	National Aeronautics and Space Administration
NCEP	National Centers for Environmental Prediction
NEXRAD	NEXt-generation RADar
NOAA	National Oceanic and Atmospheric Administration
NWP	Numerical Weather Prediction
PDF	Probabilistic Distribution Function
PILOT	upper wind observations over a land station
rms	root mean square error
RTTOV	Radiative Transfer for Television Infrared Orbiting Satellite (TIROS) Operational Vertical Sounder (TOVS)
stdv	standard deviation
TB	brightness temperature
TCWV	total column water vapour
TEMP	upper-level temperature, humidity and wind report from a land station
TRMM	Tropical Rainfall Measuring Mission
ZmVar	Z (reflectivity) Model for Variational assimilation of ECMWF

References

Baldwin, M. E. and K. E. Mitchell, 1996: The NCEP hourly multi-sensor U.S. precipitation analysis, in *Preprints 11th Conf. on Numerical Weather Prediction, Norfolk, VA (USA), 19–23 August 1996*, pp. J95–J96.

Bauer, P., P. Lopez, A. Benedetti, D. Salmond, and E. Moreau, 2006a: Implementation of 1D+4D-Var assimilation of precipitation-affected microwave radiances at ECMWF. I: 1D-Var, *Qurt. J. Roy. Meteor. Soc.*, **132**, 2277–2306.

Bauer, P., P. Lopez, A. Salmond, D.and Benedetti, S. Saarinen, and M. Bonazzola, 2006b: Implementation of 1D+4D-Var assimilation of precipitation-affected microwave radiances at ECMWF. II: 4D-Var, *Qurt. J. Roy. Meteor. Soc.*, **132**, 2307–2332.

Benedetti, A., P. Lopez, P. Bauer, and E. Moreau, 2006: Experimental use of TRMM precipitation radar observations in 1D+4D-Var assimilation, *Qurt. J. Roy. Meteor. Soc.*, **131**, 2473–2495.

Courtier, P., J.-N. Thépaut, and A. Hollingsworth, 1994: A strategy for operational implementation of 4D-Var, using an incremental approach, *Quart. J. Roy. Meteor. Soc.*, **120**, 1367–1387.

Eyre, J. R., G. A. Kelly, A. P. McNally, E. Andersson, and A. Persson, 1993: Assimilation of TOVS radiance information through one-dimensional variational analysis, *Quart. J. Roy. Meteor. Soc.*, **119**, 1427–1463.

Fisher, M., 2004: Generalized frames on the sphere, with application to the background error covariance modelling, *Proc. Seminar on Recent Developments in Numerical Methods for Atmospheric and Ocean Modelling, Reading, UK, ECMWF*, pp. 87–102.

Fulton, R. A., J. P. Breidenbach, D. J. Seo, D. A. Miller, and T. O'Bannon, 1998: The WSR-88D rainfall algorithm, *Weather and Forecasting*, **13**, 377–395.

Gérard, E. and R. W. Saunders, 1999: Four-dimensional assimilation of Special Sensor Microwave/Imager total column water vapor in the ECMWF model, *Quart. J. Roy. Meteor. Soc.*, **125**, 3077–3101.

Lopez, P. and P. Bauer, 2007: "1D+4D-Var" assimilation of NCEP Stage IV Radar and gauge hourly precipitation data at ECMWF, *Mon. Wea. Rev*, **135**, 2506–2524.

Lopez, P. and E. Moreau, 2005: A convection scheme for data assimilation: Description and initial tests, *Quart. J. Roy. Meteor. Soc.*, **131**, 409–436.

Mahfouf, J.-F. and F. Rabier, 2000: The ECMWF operational implementation of four-dimensional variational assimilation. Part I: Part II: Experimental results with improved physics, *Quart. J. Roy. Meteor. Soc.*, **126**, 1171–1190.

Marécal, V. and J.-F. Mahfouf, 2000: Variational retrieval of temperature and humidity profiles from TRMM precipitation data, *Mon. Wea. Rev.*, **128**, 3853–3866.

Marécal, V. and J.-F. Mahfouf, 2002: Four-dimensional variational assimilation of total column water vapour in rainy aeras, *Mon. Wea. Rev.*, **130**, 43–58.

Phalippou, L., 2005: Variational retrieval of humidity profile, wind speed and cloud liquid-water path with the SSM/I: Potential for numerical weather prediction, *Quart. J. Roy. Meteor. Soc.*, **131**, 409–436.

Rabier, H., F.and Järvinen, E. Klinker, J.-F. Mahfouf, and A. Simmons, 2000: The ECMWF operational implementation of four-dimensional variational assimilation. Part I: Experimental results with simplified physics, *Quart. J. Roy. Meteor. Soc.*, **126**, 1143–1170.

Rodgers, C. D., 2000: Inverse methods for atmospheric sounding. Theory and practice. *Series on atmospheric, oceanic and planetary physics*, Vol. 2, World Scientific, Singapore, New Jersey, London, Hong Kong, 238 pp.

Tompkins, A. and M. Janisková, 2004: A cloud scheme for data assimilation: Description and initial tests, *Qurt. J. R. Meteor. Soc.*, **130**, 2495–2517.

van der Grijn, G., 2002: Tropical cyclone forecasting at ECMWF: new products and validation, ECMWF Technical Memorandum 386, 13 pp.